mm-Astronomy: a review of (sub)mm band science and instruments in the ALMA era

Marcella Massardi

INAF- Istituto di Radioastronomia

Italian node of European ALMA Regional Centre

SISSA – May 2019

EUROPEAN ARC

ALMA Regional Centre || Italian

Outline

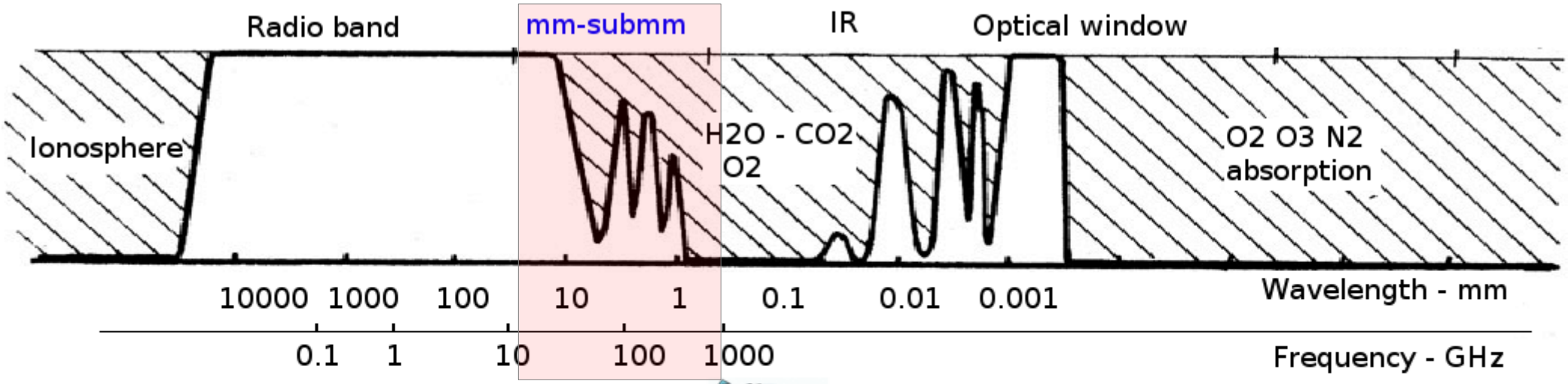

Observing instruments: **Interferometers (ALMA)**

Signals in the (sub)mm bands

Science cases parade

Observing processes: **Proposals, archives & images**

How to extract science from images: hands-on tutorial

Thermal sources

The brightness distribution for a black body in thermal equilibrium with the medium is a Planckian

$$B_\nu(T) = \frac{2h\nu^3}{c^2}\frac{1}{e^{h\nu/kT}-1}$$

In **Rayleigh-Jeans regime**

$$h\nu \ll kT$$

$$\frac{\nu}{\mathrm{GHz}} \ll 20.84\left(\frac{T}{\mathrm{K}}\right)$$

In RJ brightness is proportional to temperature

$$B_{\mathrm{RJ}}(\nu,T) = \frac{2\nu^2}{c^2}kT$$

Thermal sources in (sub)mm are in RJ regime

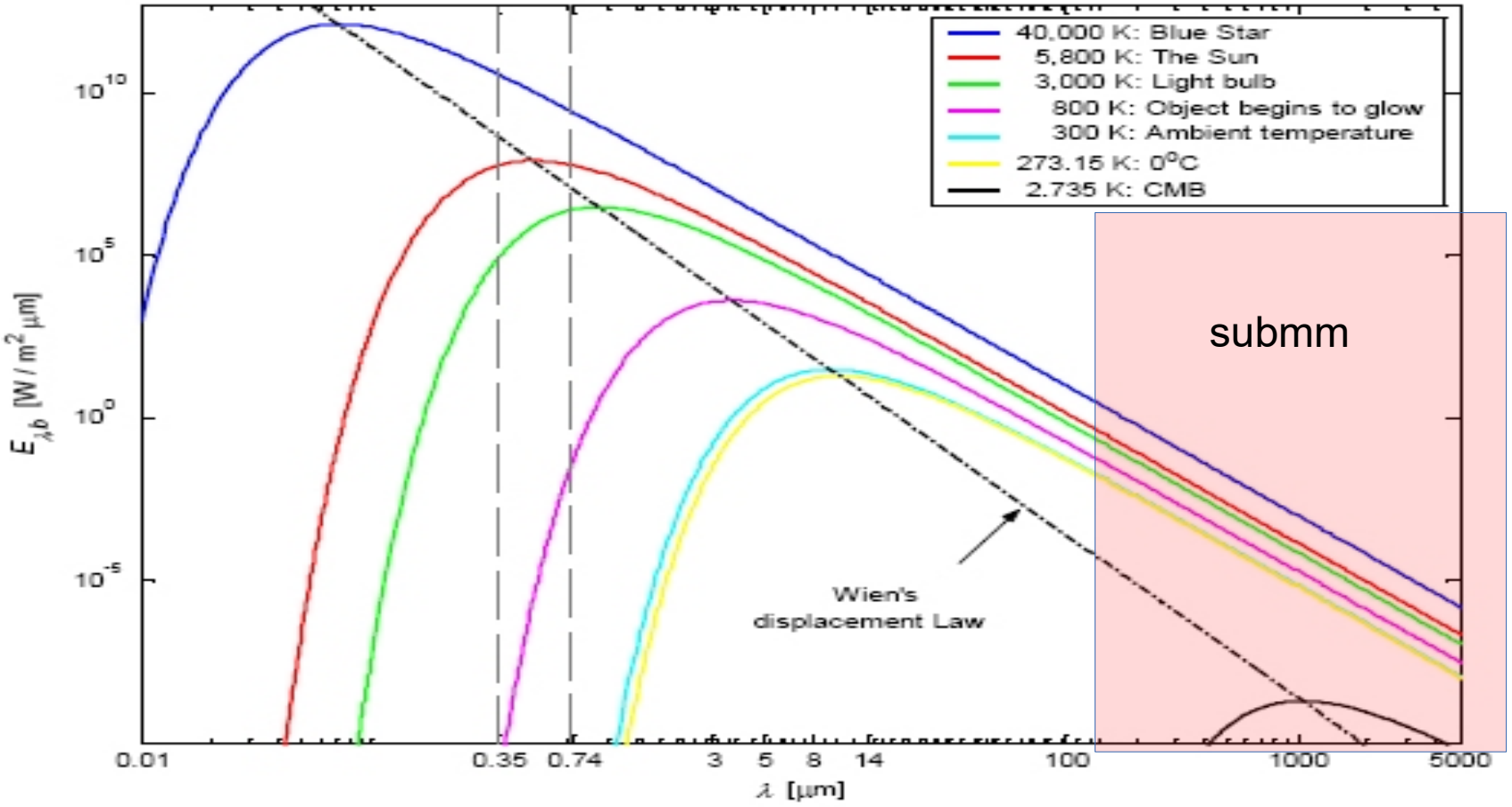

CMB

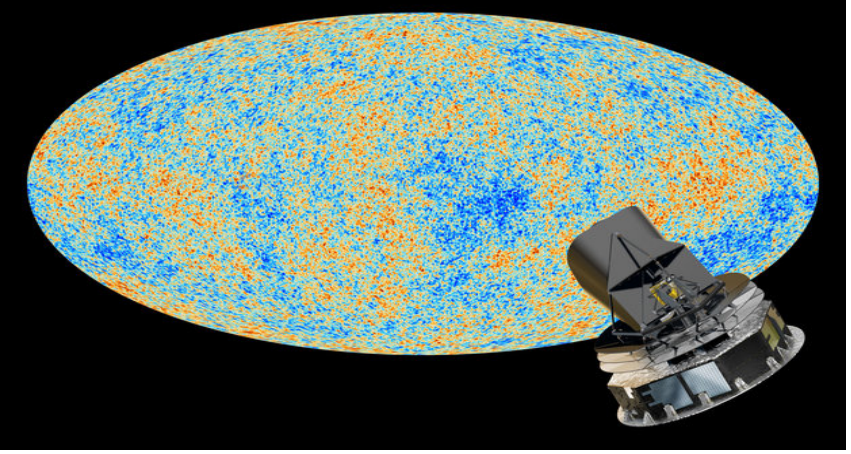

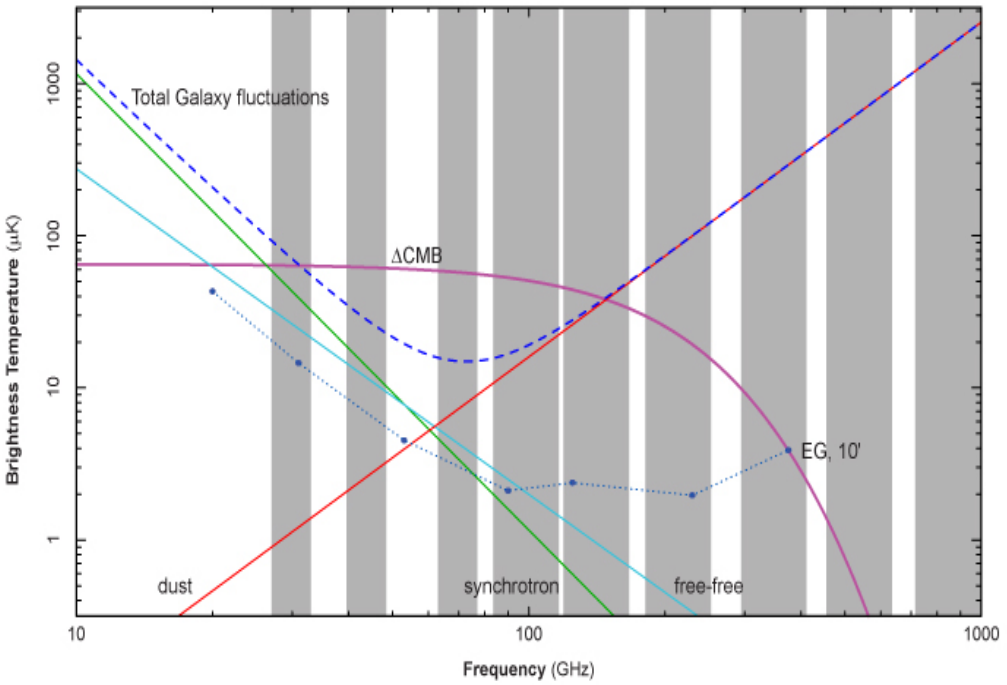

Radiation permeating all the universe at 2.726K
Hence peaking at ~163 GHz
The millimetric band is a cosmologic window because **at the minimum of the intervening foregrounds between the CMB and us.**
Point EG sources are the major contaminant to scales smaller than 30 arcmin.

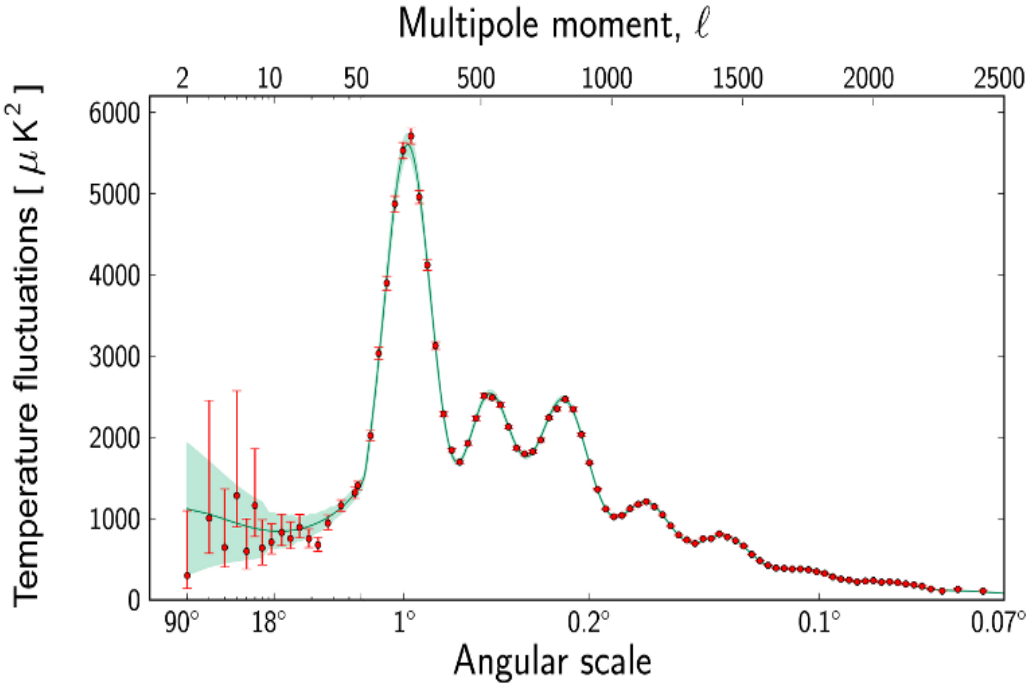

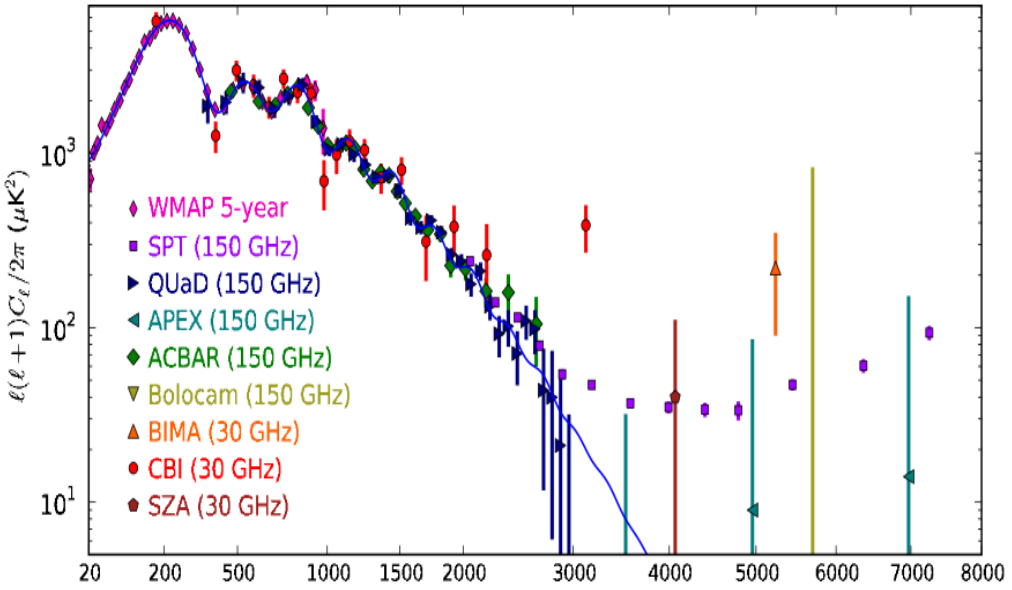

(Fowler et al. 2010, Planck collaboration 2013)

CMB

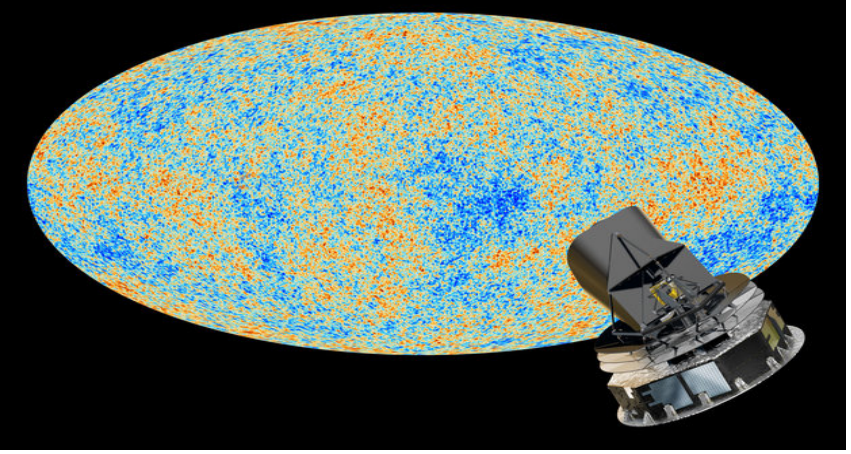

Radiation permeating all the universe at 2.726K
Hence peaking at ~163 GHz
The millimetric band is a cosmologic window because **at the minimum of the intervening foregrounds between the CMB and us.**
Point EG sources are the major contaminant to scales smaller than 30 arcmin.

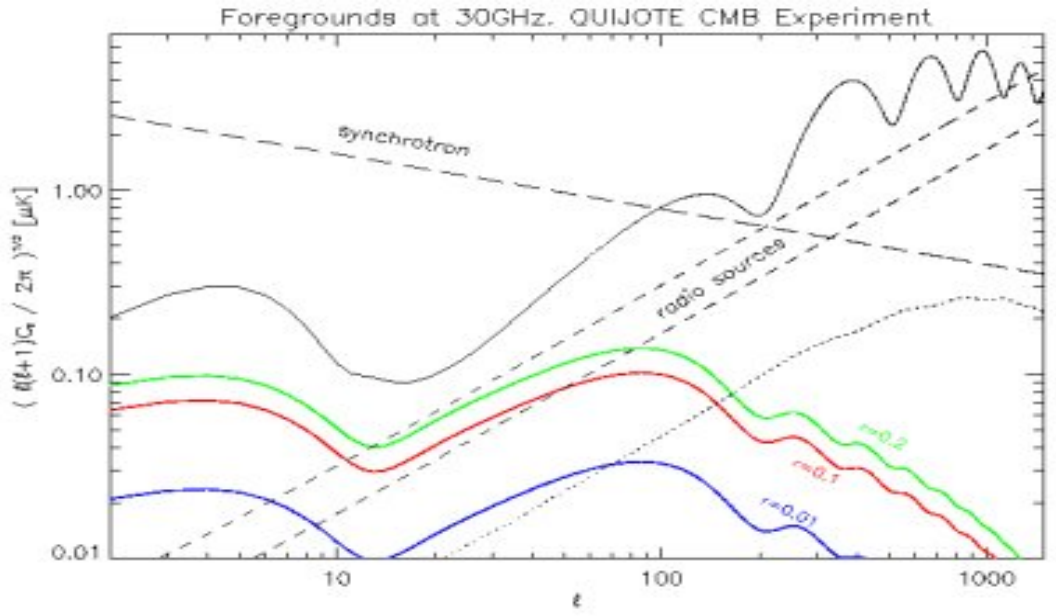

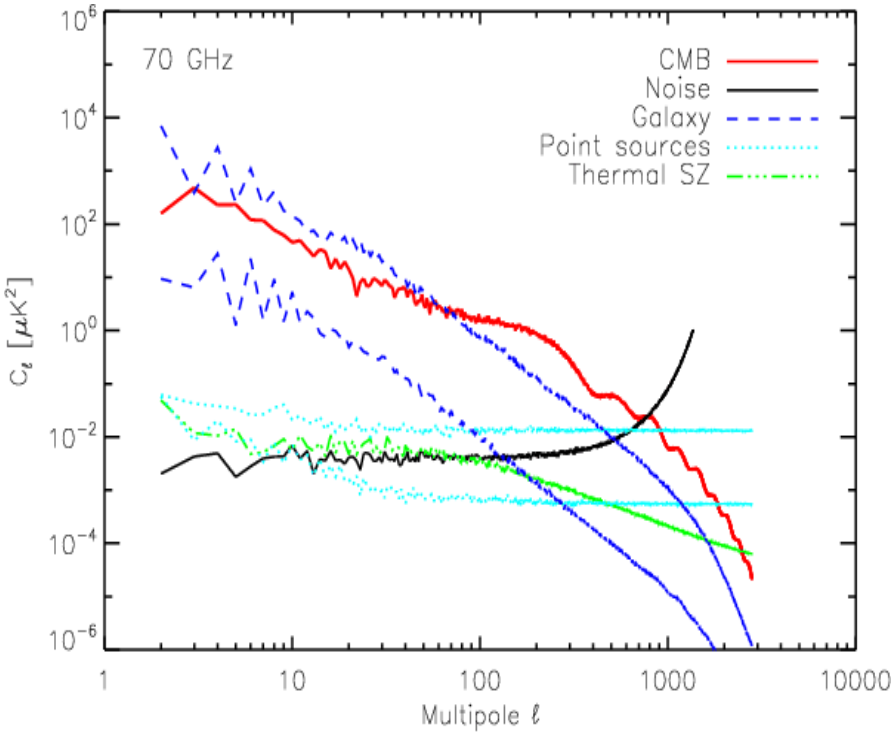

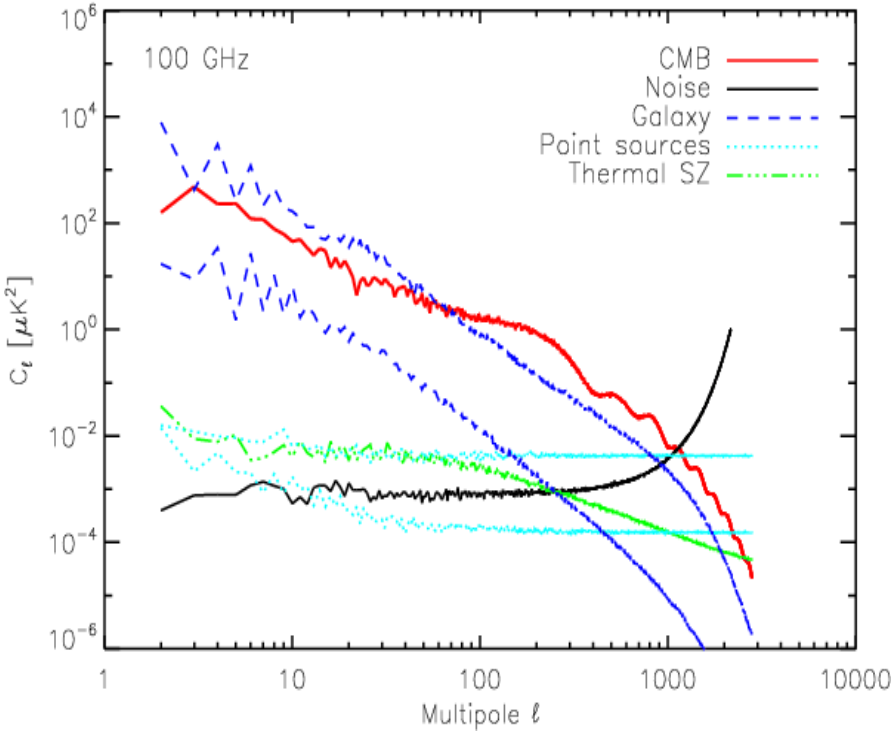

(QUIXOTE website, Leach et al. 2008)

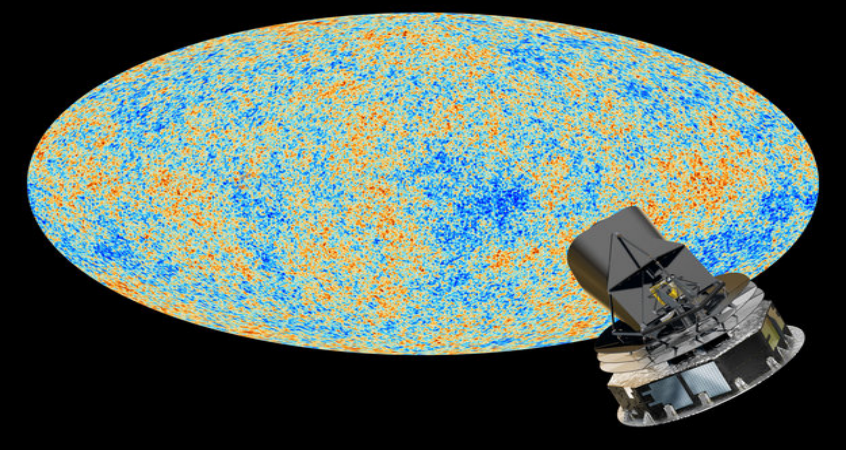

A signal jam

Planck gave us a summary of what we should expect in the (sub)mm bands:
syncrotron, dust emission, and spectral lines

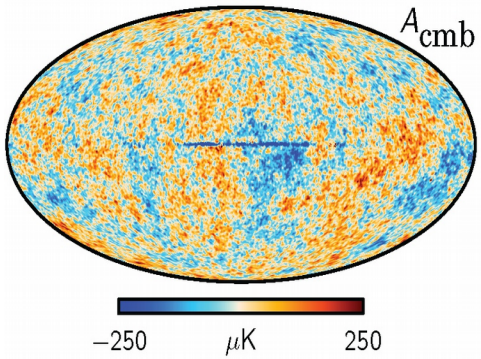

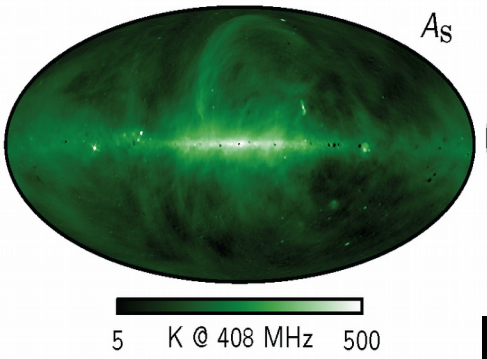

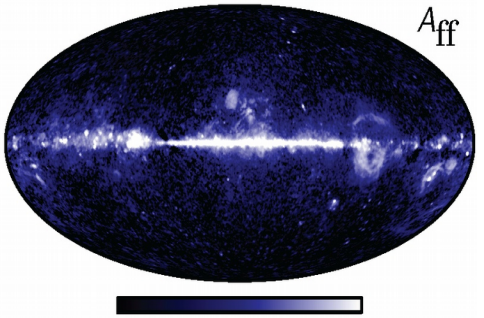

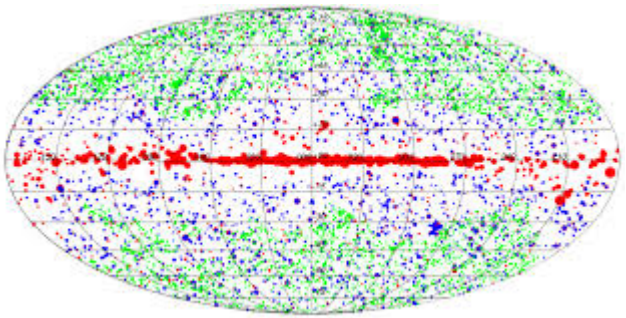

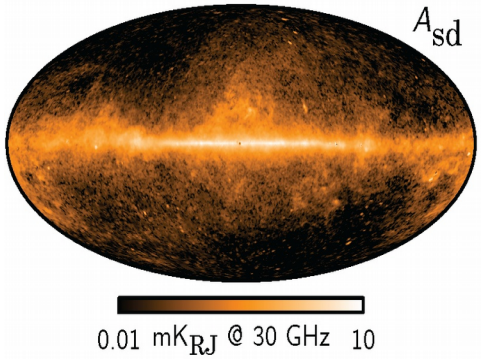

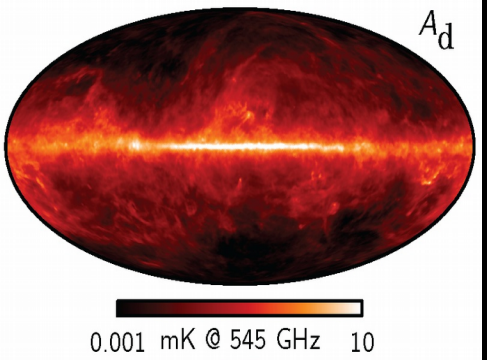

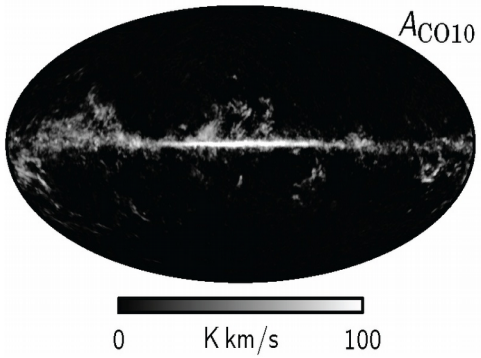

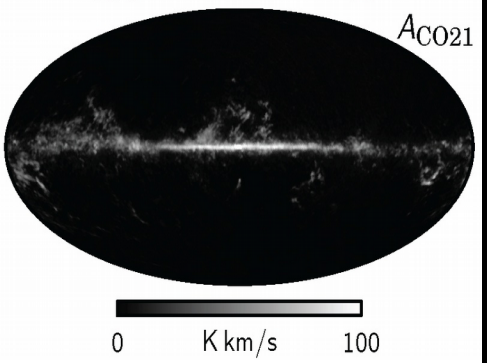

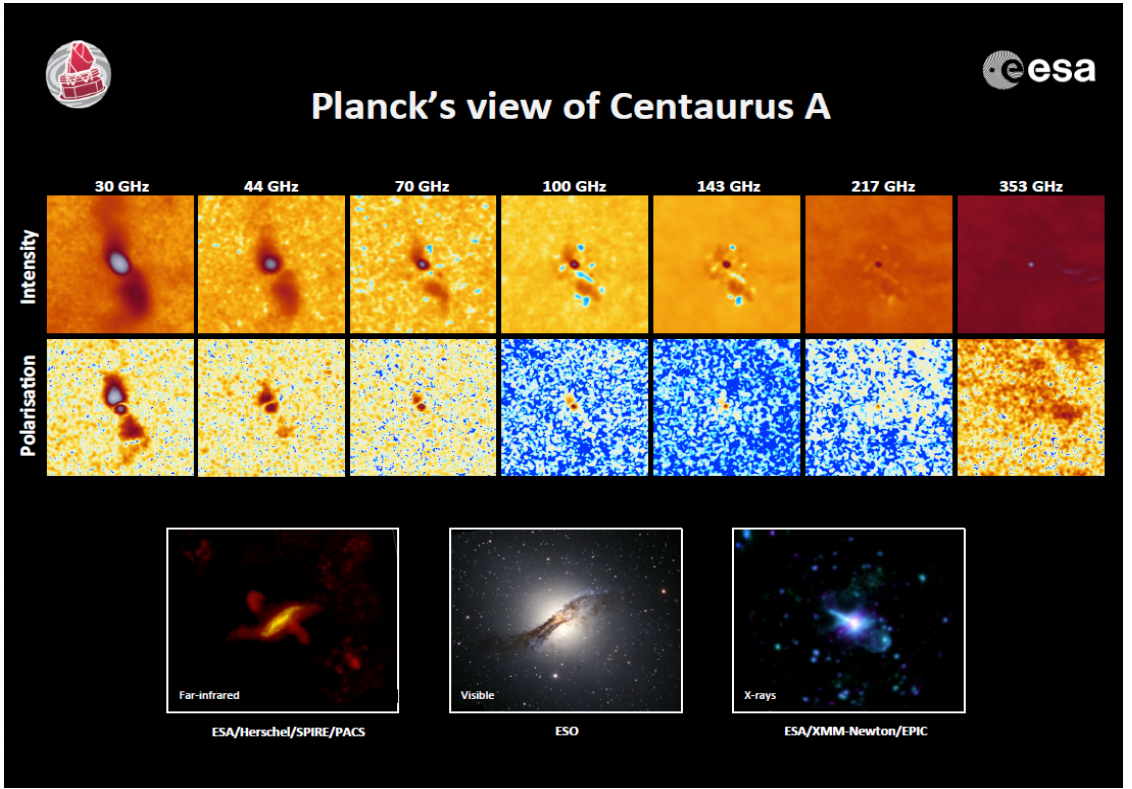

Need high resolution

Herschel showed us the structure of the emission:
a detailed view is needed to trace the origin
of the emission for each signal

Credits: INAF/ESA Herschel Space Observatory/Hi-GAL Consortium/ASI; Map-Making by UNIMAP (L.Piazz

Different approaches to observations

Single Band

- only one signal,
  tracer of a physical behaviour

Multi frequency

- matching several tracers for
  a complete overview

Single object

- a peculiar object or
  a representative object
- useful to enter into
  details of mechanisms

Statistical population analysis

- collect statistically significant
  Samples/ Surveys
- less detailed but more general for
  info to modeling and scenarios

Overview of a galaxy

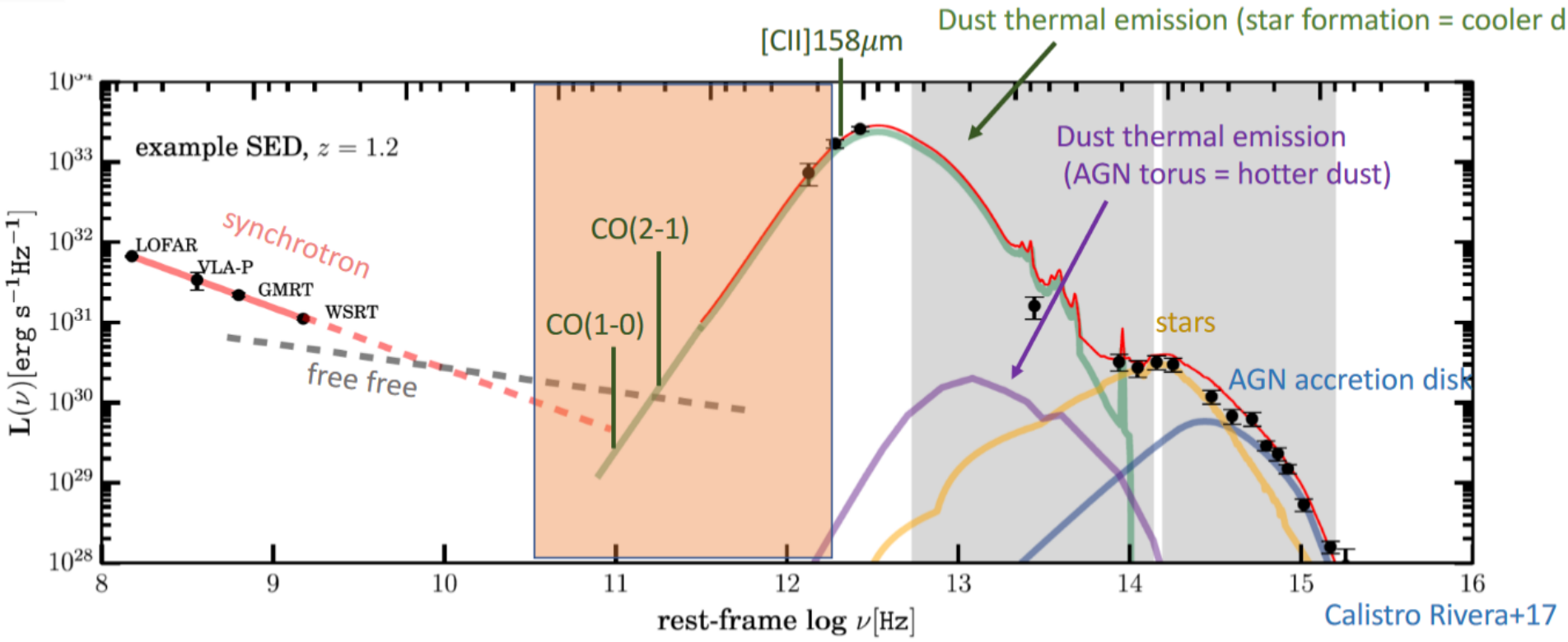

ALMA windows
(Bands 1 -11)

Spectral energy distribution (SED) of a dusty star forming galaxy with an AGN

Synchrotron

Synchrotron emission is caused by emission from relativistic electrons spiralling in magnetic fields.
The radiation emitted is confined to a beam pointing In the direction of the motion of the particle
It is also polarized in the plane perpendicular to the magnetic field, with the degree and orientation of the polarization providing information about the source magnetic field.

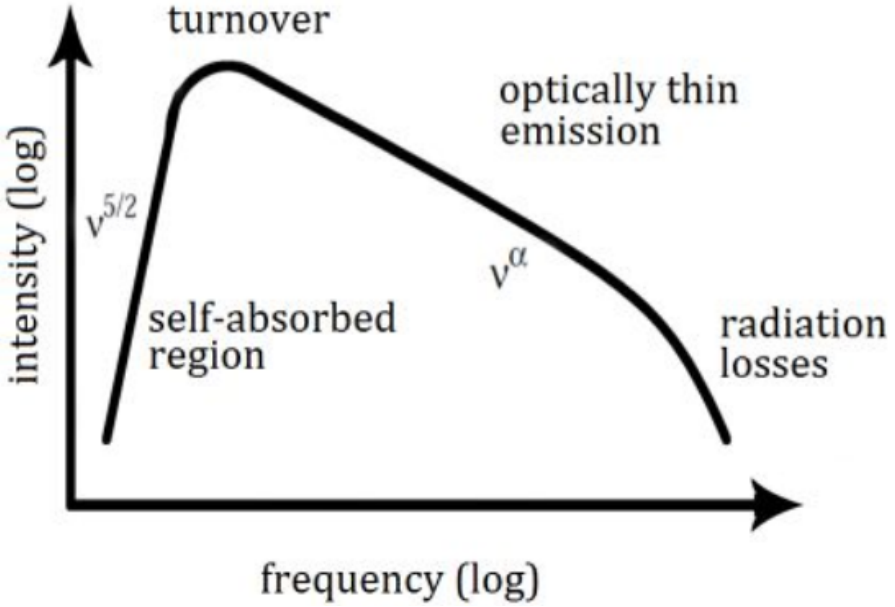

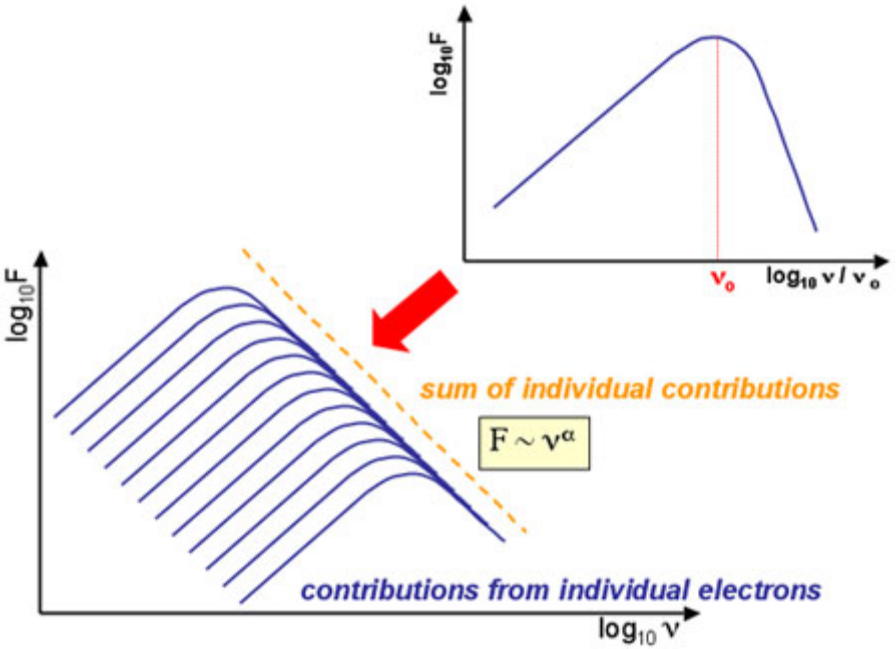

$$\alpha(\nu_1, \nu_2) = \frac{\log(S_1/S_2)}{\log(\nu_1/\nu_2)}$$ **Spectral index**

AGN

AGNs generally heat their circumnuclear dust to temperatures much higher than starburst galaxies.
The far-IR and submm emission is a combination of synchrotron from the magnetic fields associated with the BH in the jets and with the star formation in the host galaxies, even in powerful QSOs.

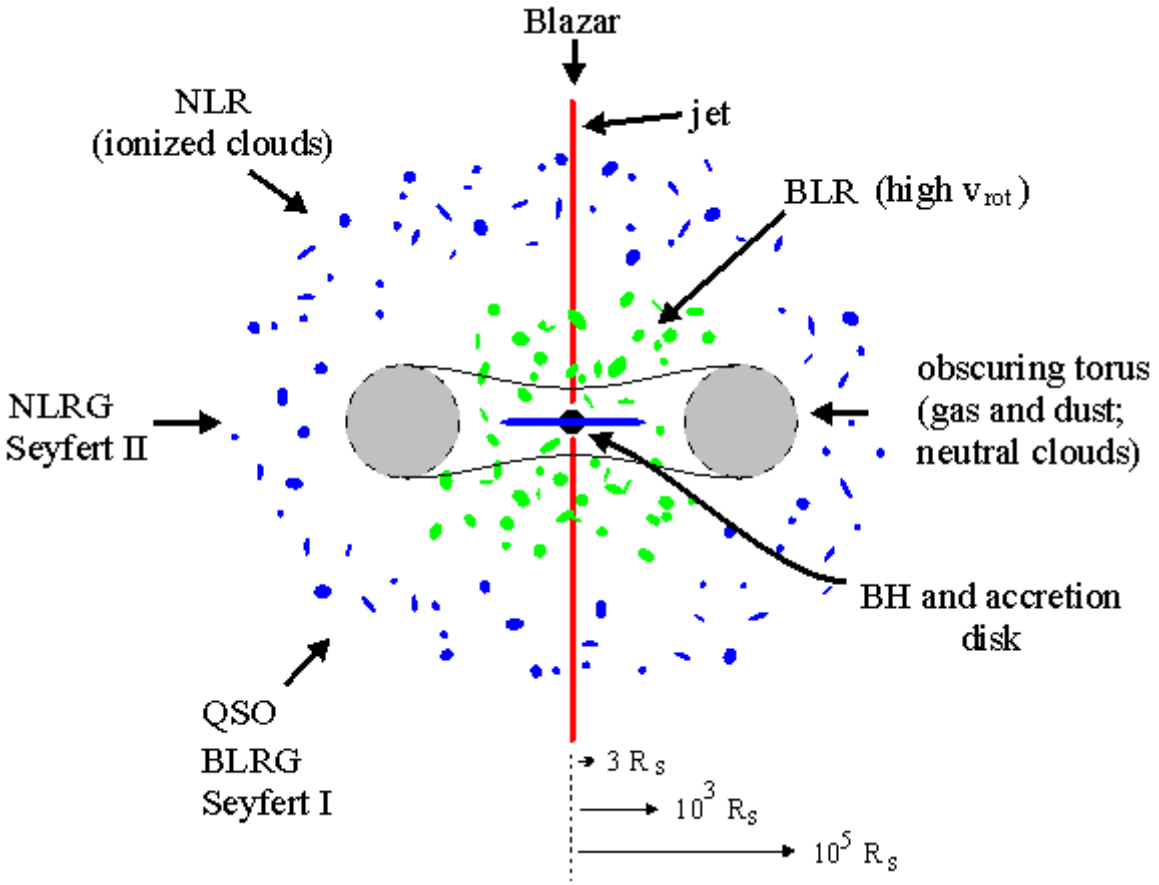

NOTES on SCALES

BLR< 0.1pc
(velocities $10^{3\text{-}4}$km/s)
Torus 1-5 pc
NLR 100 pc
Jet <1Mpc

An ALMA resolution element (10marcsec @300 GHz) Corresponds to
@z=0.1 10pc
@z=0.5-3 40-60pc

In CenA (z=0.018) → 0.4pc
In NGC1068 (z=0.037) → 0.8pc

Synchrotron in AGN

Synchrotron emission is associated to jets in AGN.
Spectral Energy distribution (SED) is a combination of

- **combination of multiple synchrotron components** along the jets with peak at the higher frequencies the more energetic is the emitted photons (i.e. the stronger is the magnetic field = the closer to the BH). More energetic photons are also less absorbed (i.e. electron clouds are less thick). Combined spectra are flatter than the spectra of single components

Steep spectra = synchrotron optically thin emitted
Flat spectra = synchrotron self-absorbed multiple components

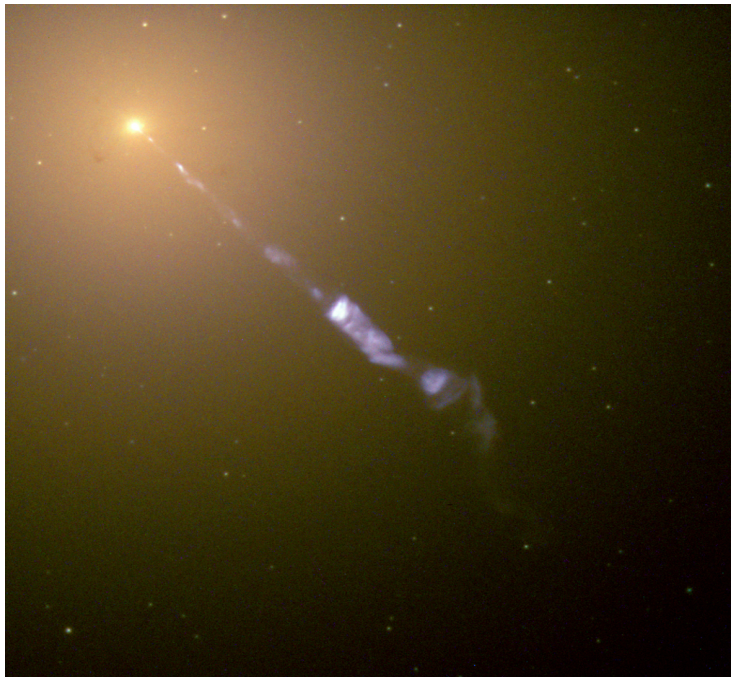

- **Doppler boosting** due to relativistic beaming effects that enhances the flux as $S_r = S_e D^{3-\alpha}$ so that in the optically thin regime the flux density increases more than in the thick range.

At higher frequencies the signal is less absorbed and boosted, so the bright samples are dominated by flat spectra sources.

The self-absorbed components are frequently unstable, young and rapidly evolving. Variability affects source counts (we detect more easily high states), SEDs and extrapolations.

Synchrotron in AGN

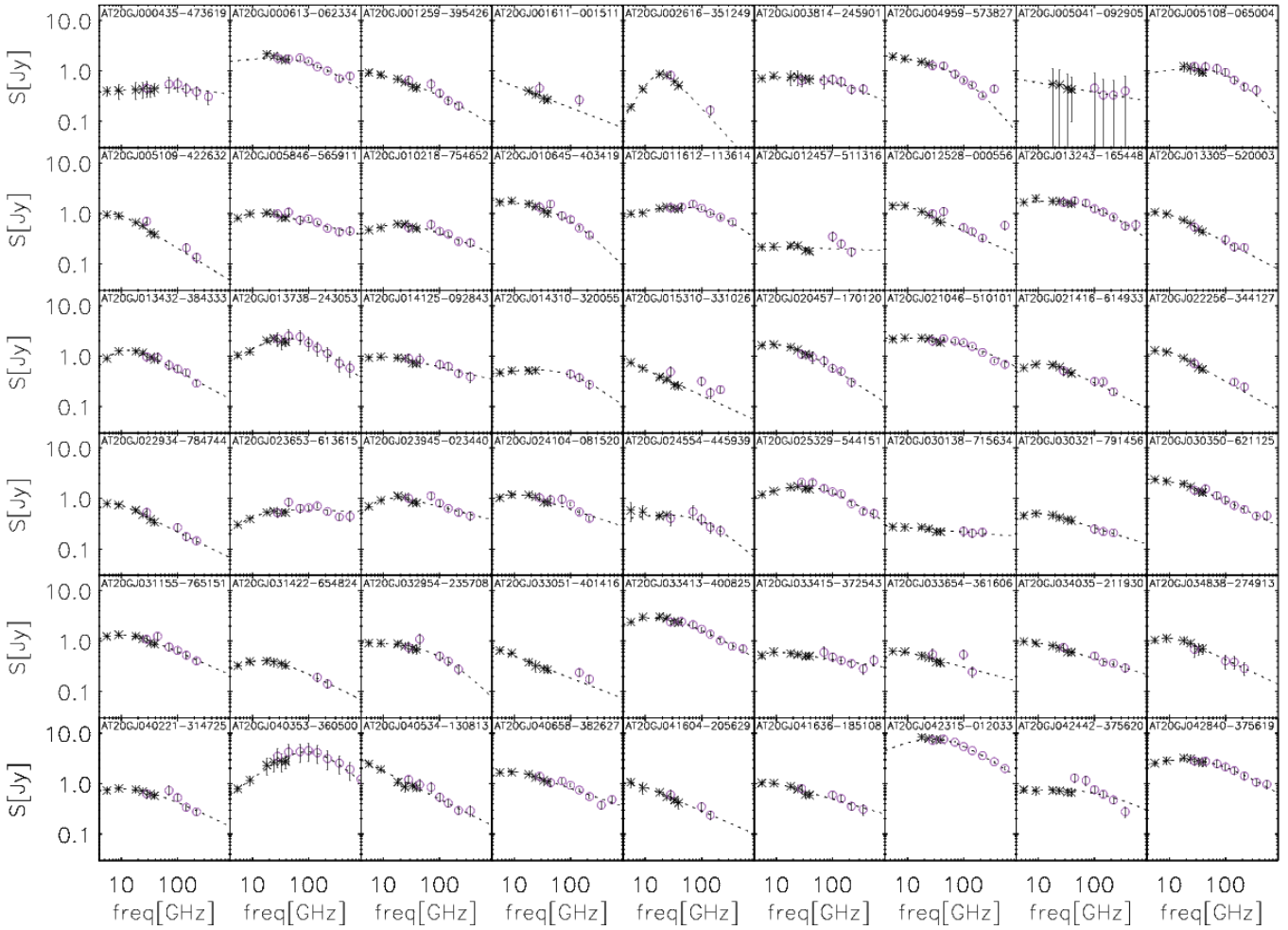

Radio colour-colour plot

(comparison between spectral indices)

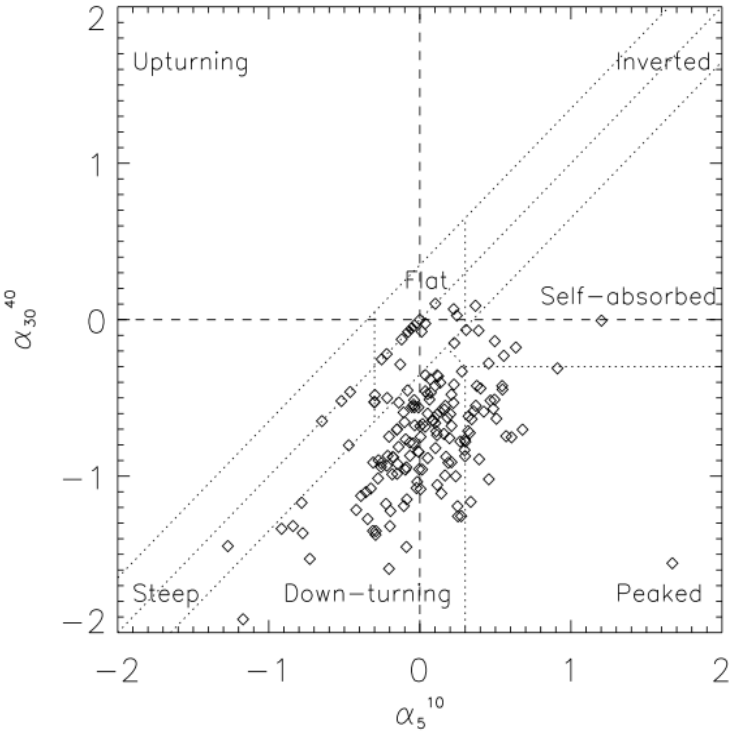

Type	$200 \leq S_{20\,\mathrm{GHz}} < 500$ mJy (per cent)	$S_{20\,\mathrm{GHz}} \geq 500$ mJy (per cent)
Flat	5.1	10.3
Steep	13.3	3.6
Inverted	0	0.6
Peaked	11.2	14.5
Downturning	65.3	66
Self-absorbed	5.1	4.8
Upturning	0	0

Down-turning spectra dominate the population in the frequency range 5-40 GHz,
with an increasing fraction of steep spectra as the flux decreases.

No source shows upturning or inverted spectra

Variability trend seems to increase with frequency and time lag but not with flux density

Variability

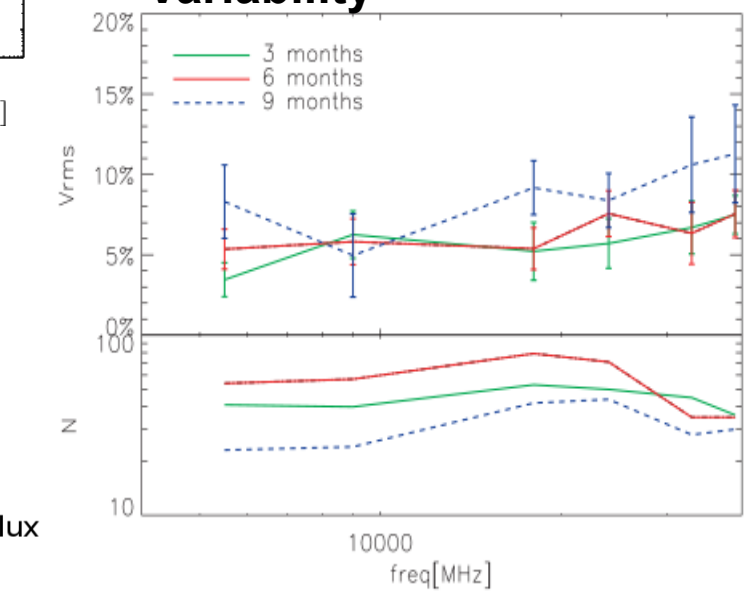

Synchrotron in AGN

As more energetic photons are also less absorbed (i.e. electron clouds are less thick) the inner and denser regions of the AGN become less optically thick and become more easily observable as the frequency of observation increases.

Hence, mm observations of AGN provide information on the jet structure and unveil the details of their basis getting closer to the black hole.

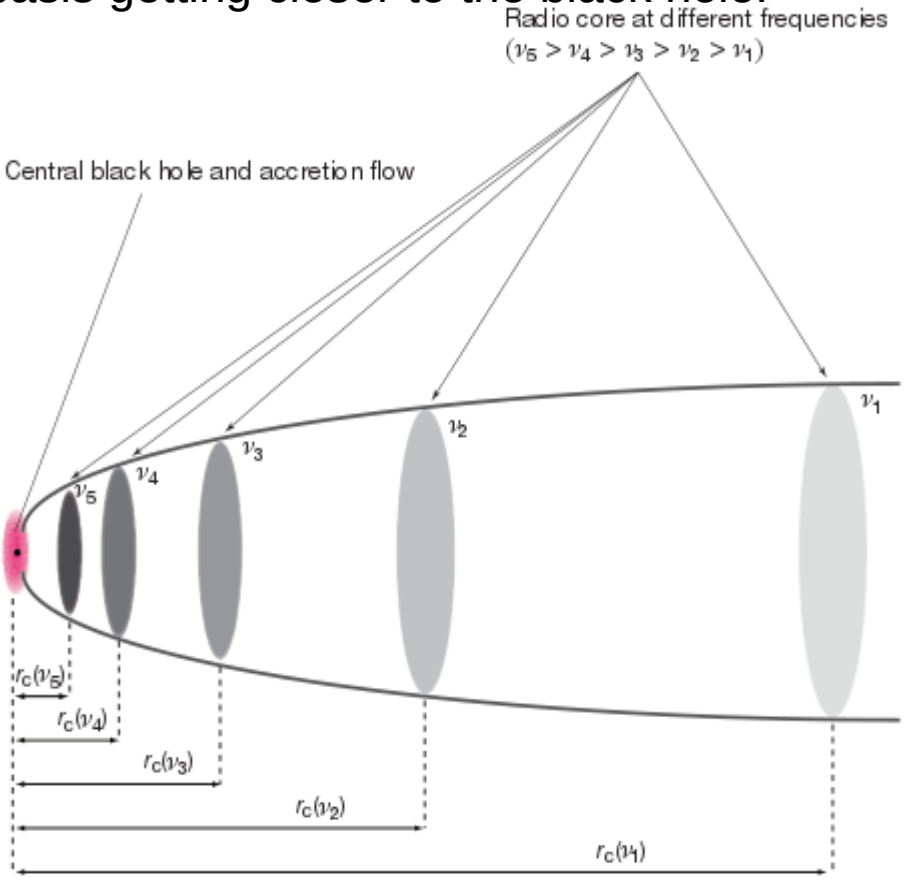

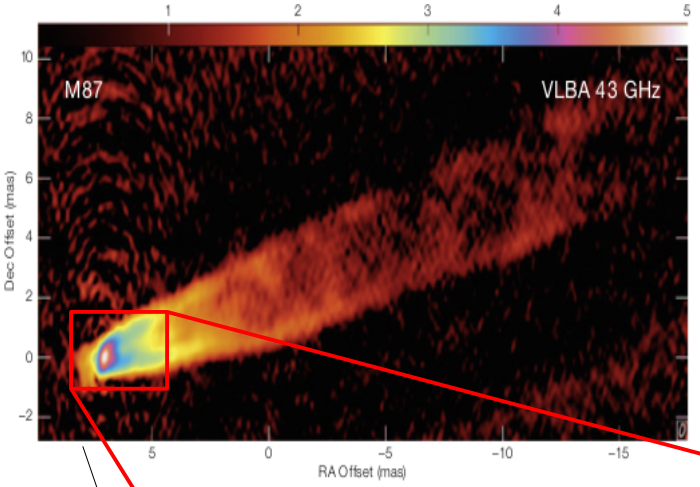

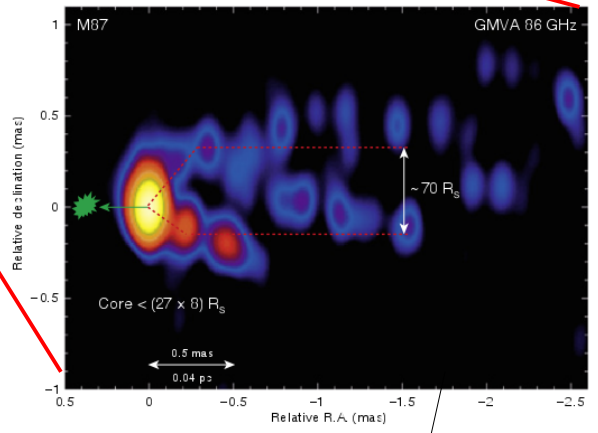

(Hada et al. 2012)

Dust

Dust grains are solid, macroscopic particles composed of dielectric and refractory materials (mostly silicates or graphites). Typical grain sizes in interstellar dust ranges between few nm to few microns.

In our Galaxy the gas-to-dust ratio is about 100:1.
(ISM is about 10% of the baryonic mass of the Galaxy -> dust is roughly 0.1% of the total)

What is the role of dust grains?

- **they scatter star light modifying the signals**
- **they absorb roughly 30-50% of the starlight emitted by the Galaxy**
- **re-radiate it as far-infrared continuum emission**
  (1/3-1/2 of the bolometric luminosity of the Galaxy!)
- **are the primary sites of molecular formation, and play the catalyst role**
  (all of the H2 in the ISM form on grains).

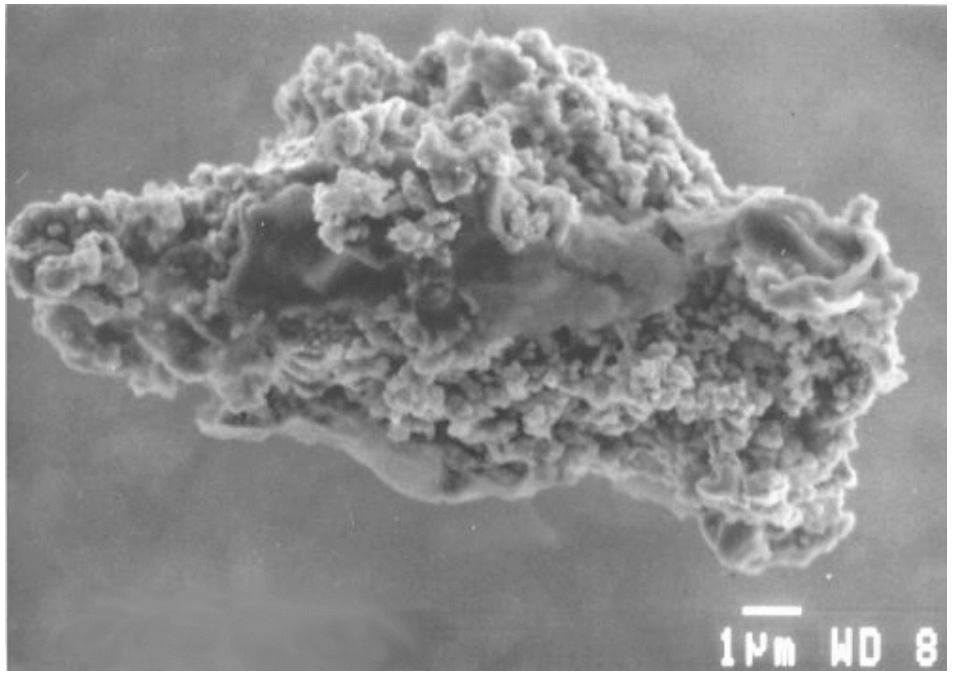

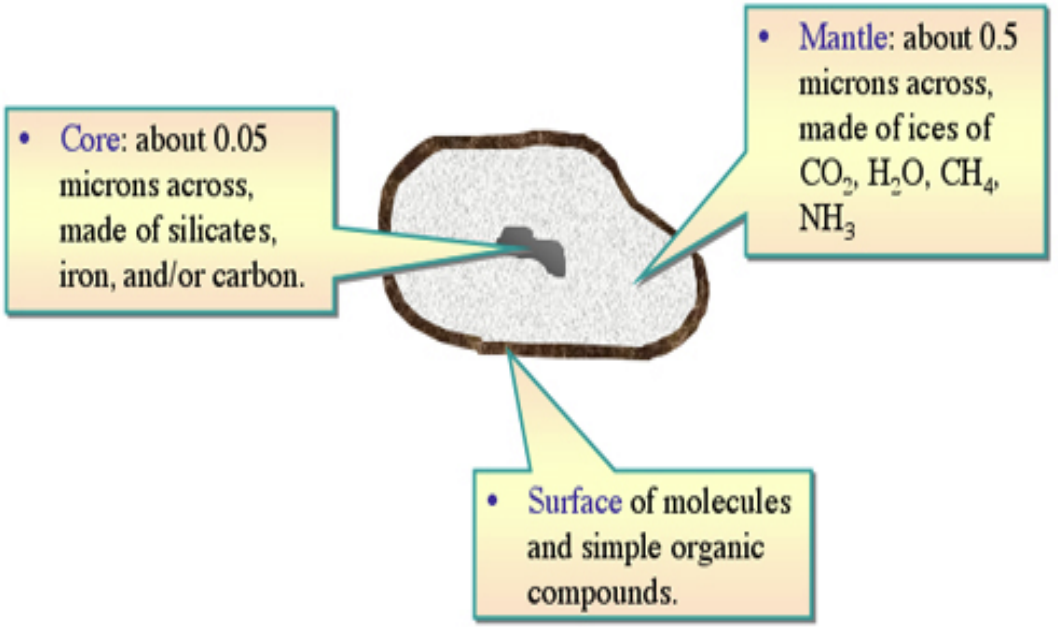

Dust scattering

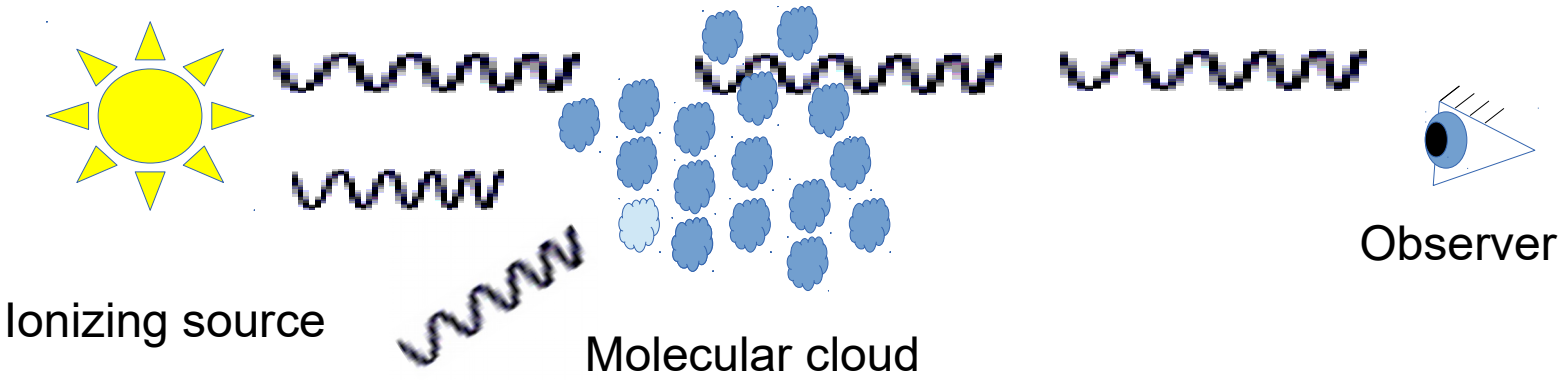

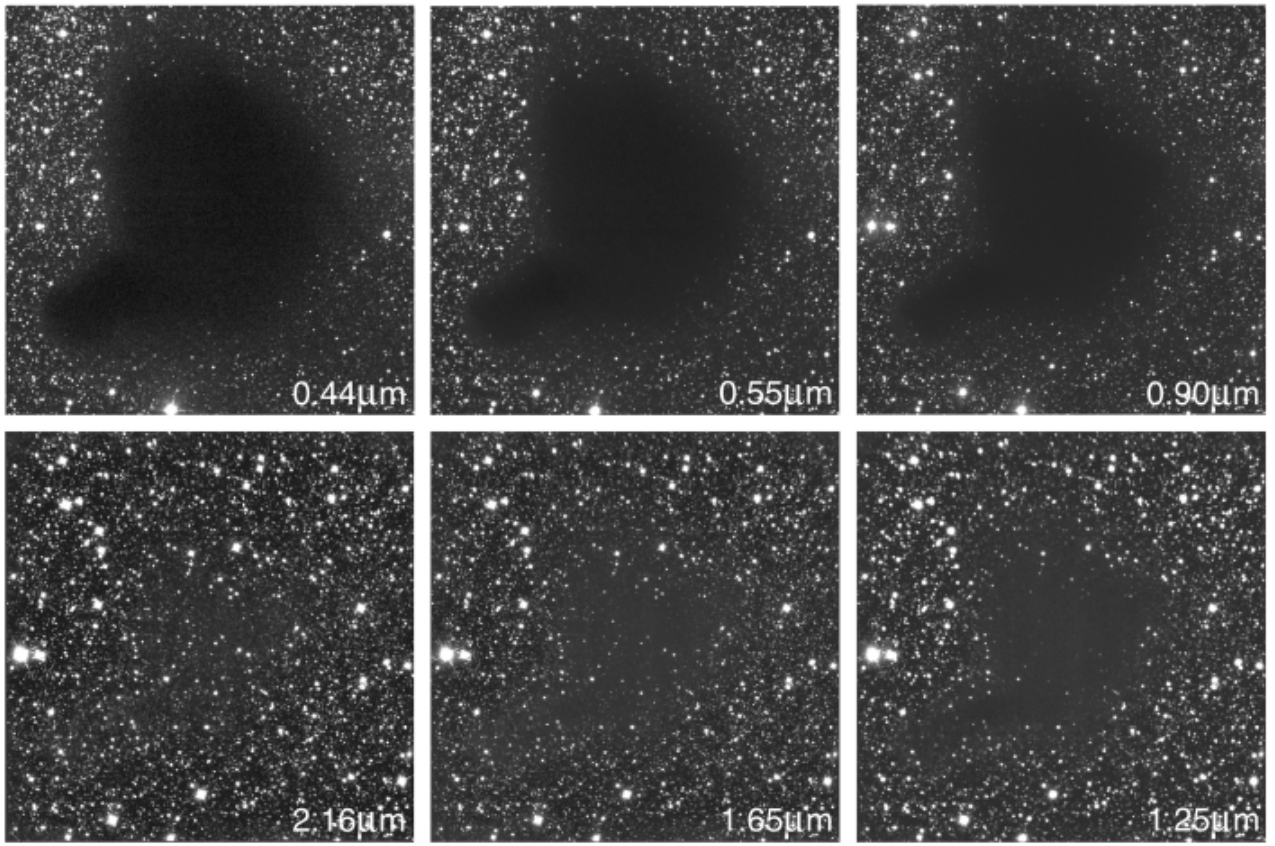

The Dark Cloud B68 at Different Wavelengths (NTT + SOFI)

Our view is blocked in visible light because the dust grains are about the same size as optical wavelengths - about one micron or less - and so are very effective at scattering or absorbing that light.
But longer infrared wavelengths undulate around the dust.
The longer the wavelength, the thicker the layer of dust it can penetrate.
So sub(mm) radiation can move freely through the Universe, unobstructed by dust.

Dust emission

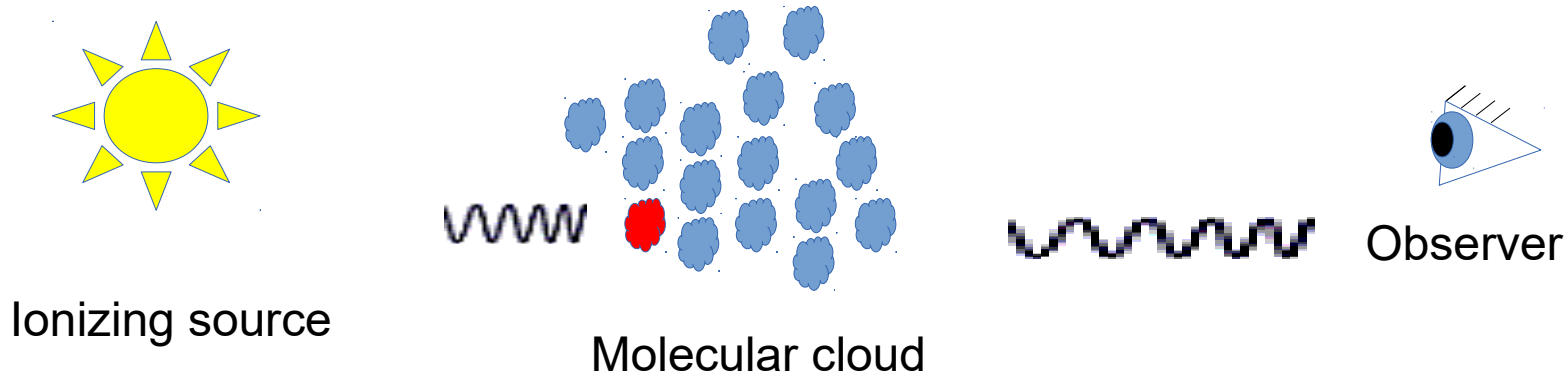

Graphite and silicate dust grains absorb opt-UV radiation and heats up (photoionization).

The visible and ultraviolet light that the dust absorbs warms the grains just enough for them to re-radiate the light at sub(mm) wavelengths. The colder the grains, the longer the wavelength of emission.

Evolved stars (e.g. ages above 100–200Myr) contribute significantly to the dust heating, which tends to cause the IR luminosity to overestimate the SFR. The fraction of dust heating from young stars varies by a large factor among galaxies: **in extreme circumnuclear starburst galaxies or individual star-forming regions, nearly all of the dust heating arises from young stars, in evolved galaxies with low specific SFRs, the fraction can be as low as~10%.**

Dust grains show linear polarization, which leads to the conclusion that grains are elongated and aligned by magnetic fields. The direction but not the strength of the magnetic field can be determined from dust polarization. The fractional polarization is rather small, so requires high sensitivity and care to keep instrumental effects small

Dust emission

If optical depth is small (like in mm band)

$$T = T_{\rm dust}\,\tau_{\rm dust}$$

Then the **flux is**

$$S = \frac{2\,k\,T}{\lambda^2} = 2\,k\,T_{\rm dust}\lambda^{-2}\,\tau_{\rm dust}\Delta\Omega$$

The dust optical depth is small and goes as $\lambda^{-\beta}$ with $1<\beta<2$ so that the flux density goes as λ^{-3} to λ^{-4}.

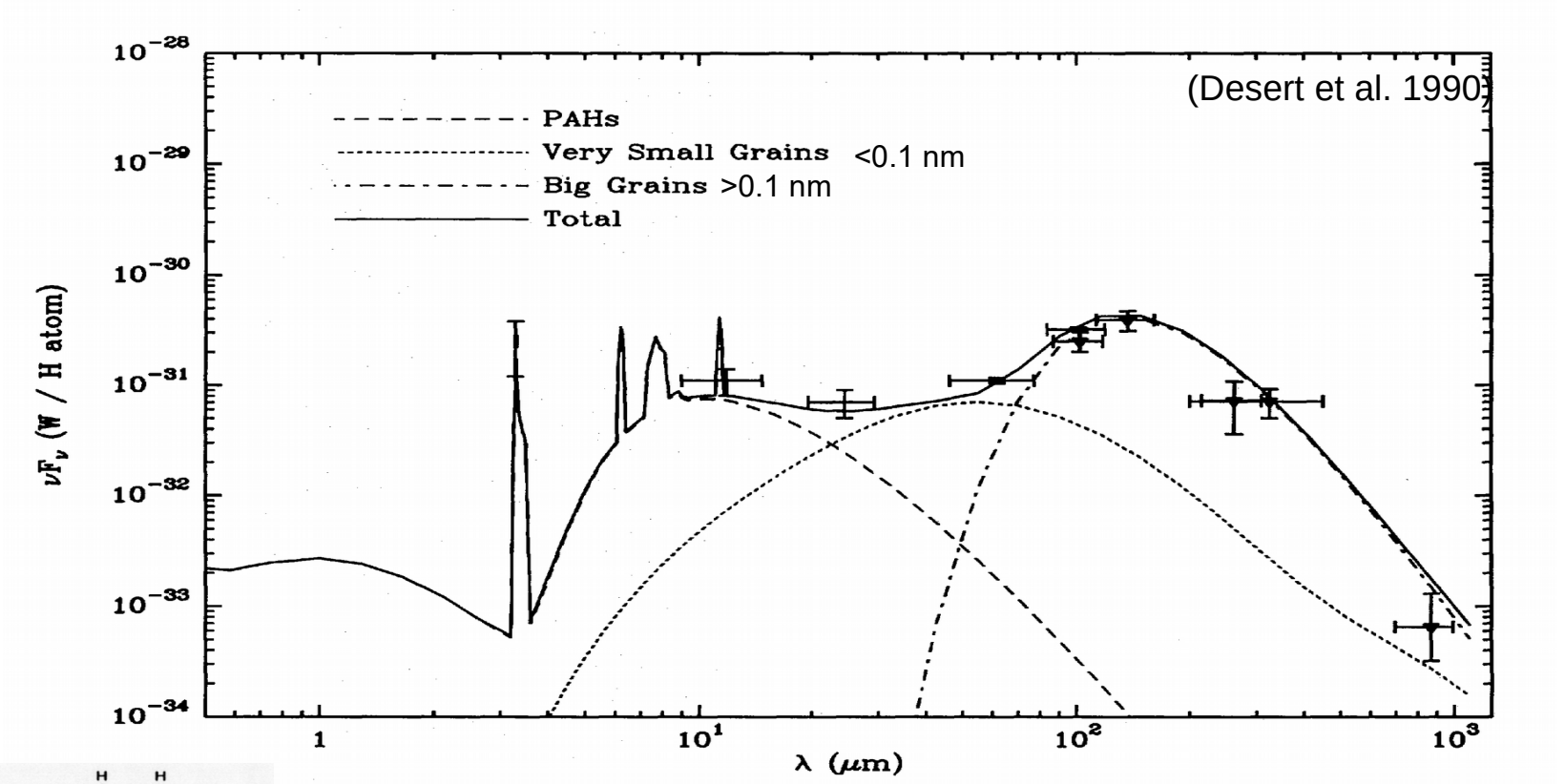

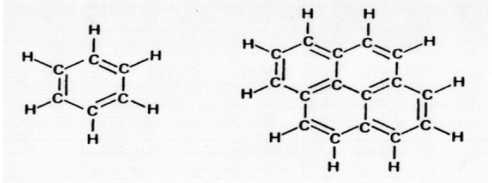

Polycyclic Aromatic Hydrocarbons are combinations of aromatic rings (e.g. benzene)

Info from the dust profiles

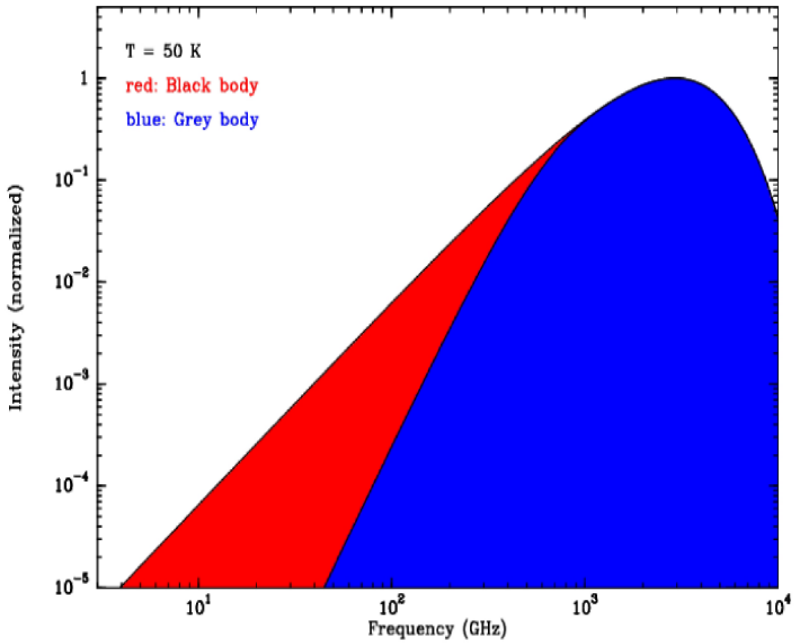

Temperature By fitting a greybody spectrum it is possible to estimate the temperature. Assumptions have to be done on the dust grain properties

$$T = T_{\rm dust}\,\tau_{\rm dust}$$

Mass Given the temperature, mass is

$$M_{\rm d} = \frac{D_{\rm L}^2 S_{\nu_{obs}}}{(1+z)\kappa_\nu B_\nu(T_{\rm d})} \qquad k_\nu \propto \nu^\beta$$

depending on the grain properties through the absorption coefficient (0.04-0.15 m2/kg at 1mm)

Photometric redshifts can be retrieved via SED fitting with template models. A degeneracy remains with temperature

(Sub)mm measurements are crucial to reconstruct the dust peak and improve the SED fitting qualities. Issues can be added by the presence of AGNs

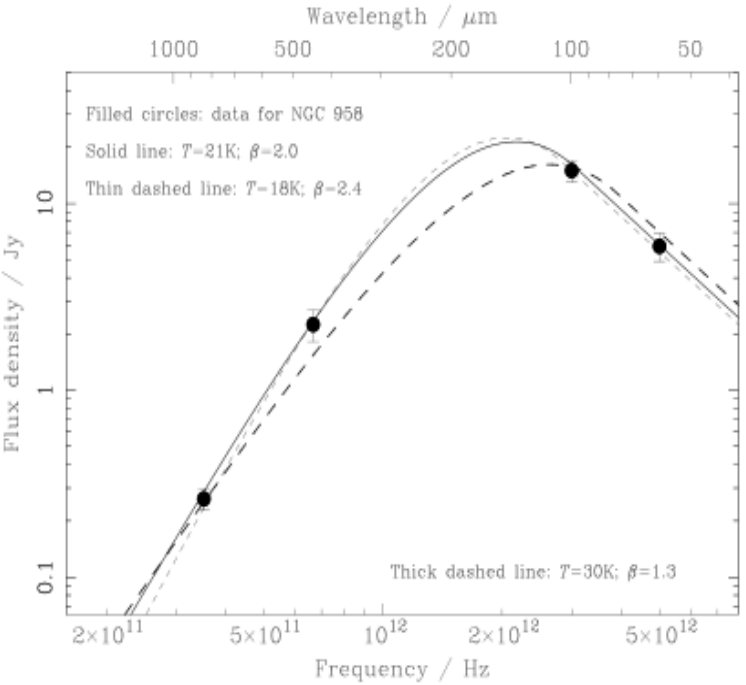

The negative k correction

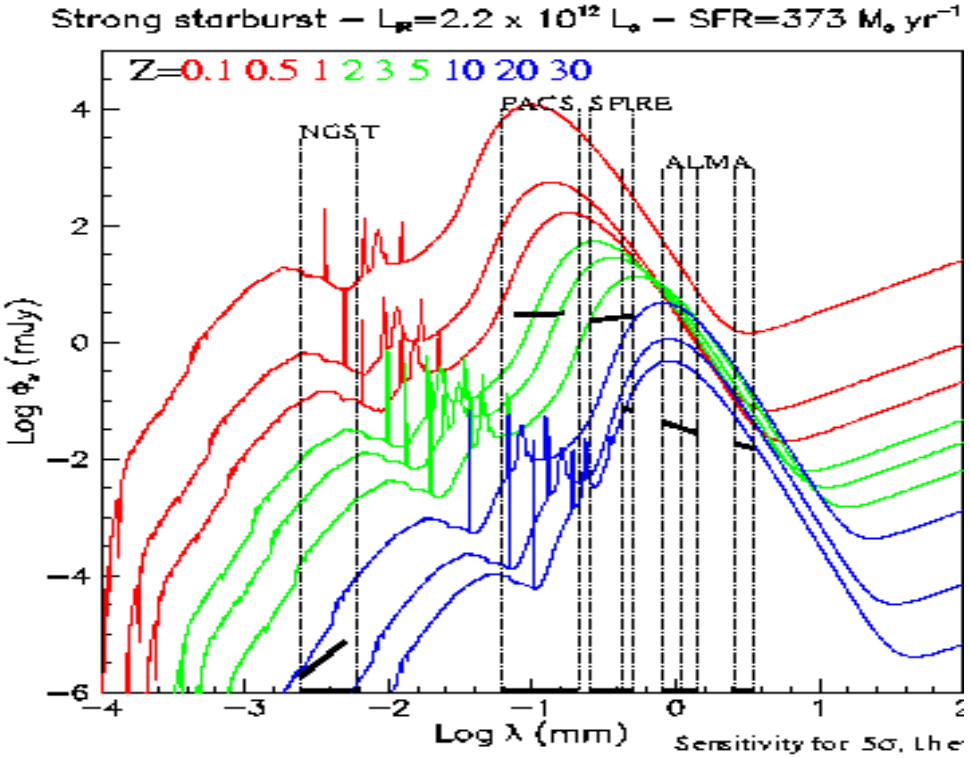

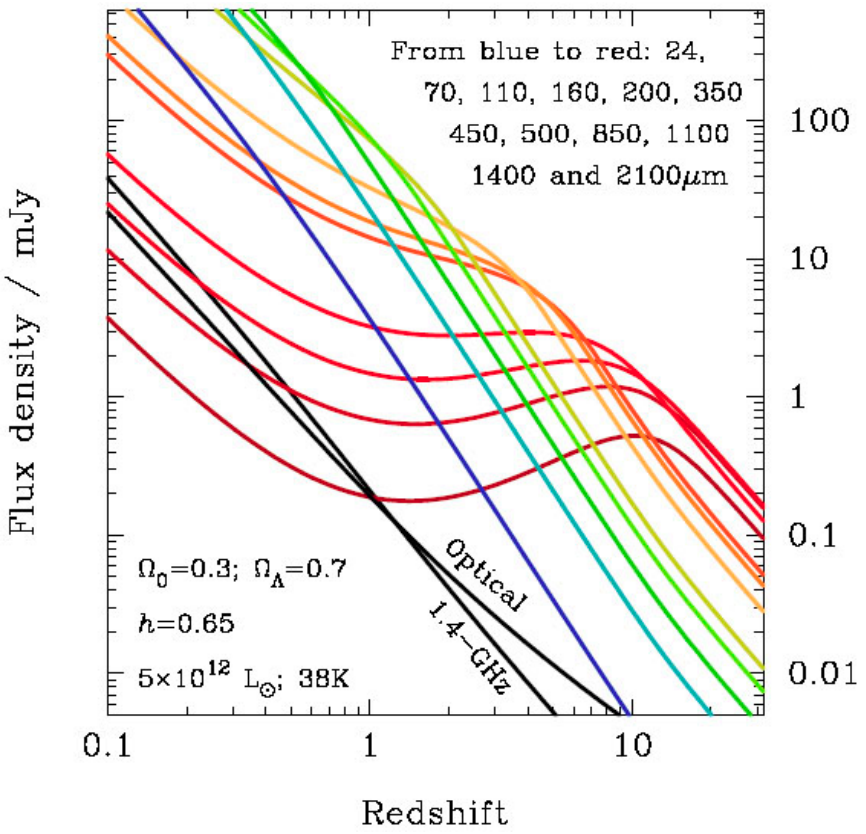

Given the dust scaling with frequency, the net effect of redshifting dust spectra is that to more than compensate the inverse square law of decreasing flux density with z
In the mm band the same dusty galaxy appear brighter at increasing redshift.
Deep mm band fields are dominated by high-z galaxies

(Blain et al. 1993, 2002)

Line transitions

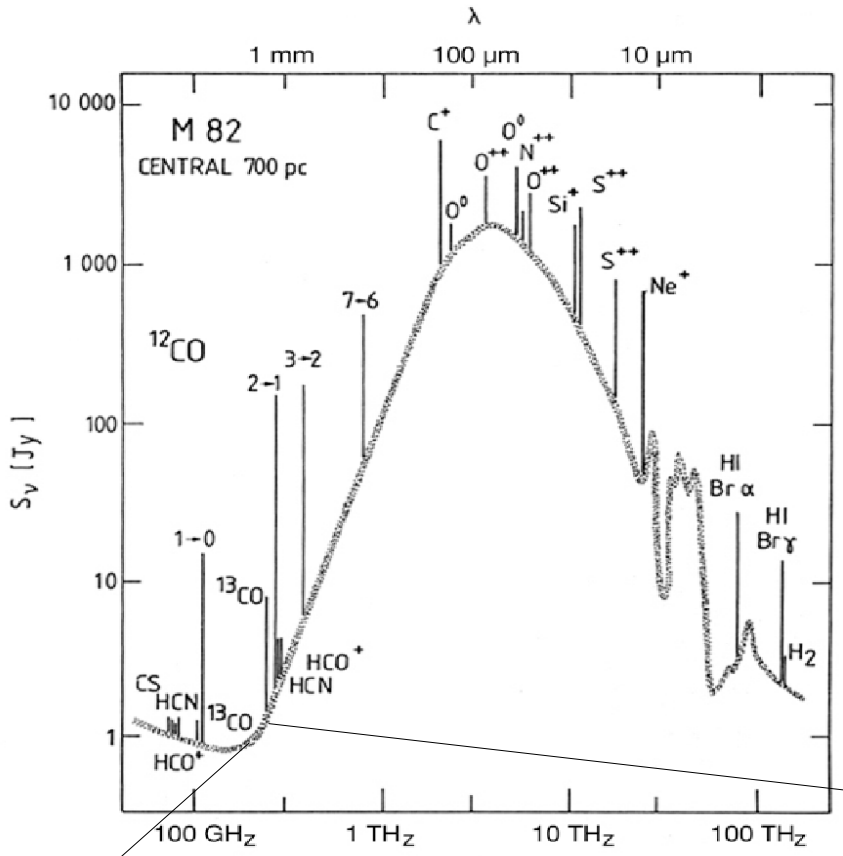

- Continuum is dominated by dust and synchrotron

- Spectra show a very rich chemistry

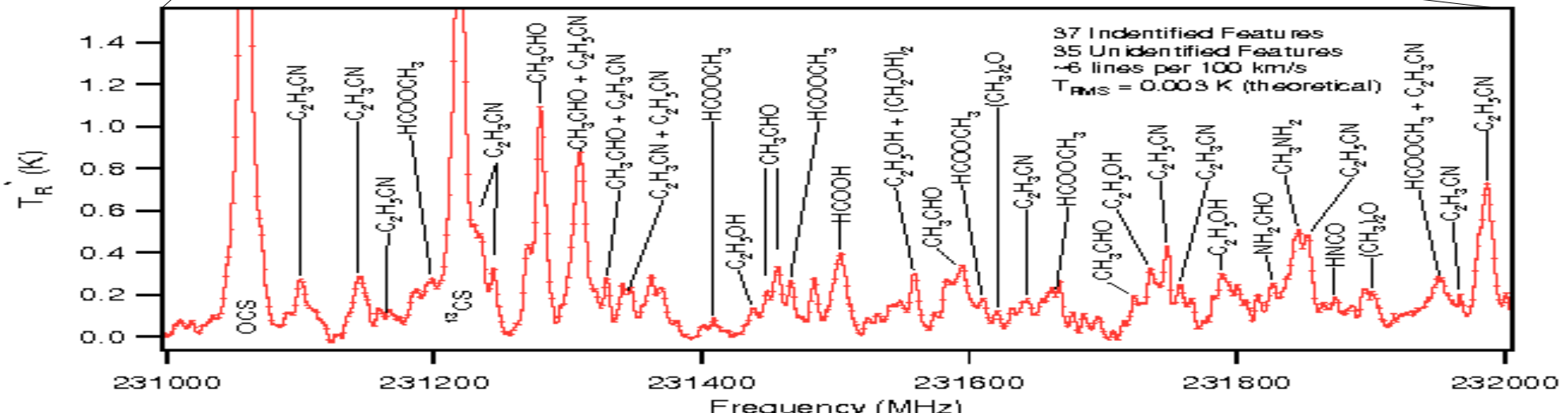

Line transitions

Transitions probability per unit time between different energetic levels can be expressed through Einstein coefficients:

A_{21} for spontaneous emission
$B_{21}U$ for induced emission (radiation)
γ_{21} for induced emission (collisions)
$B_{12}U$ for absorption (radiation)
γ_{12} for absorption (collisions)

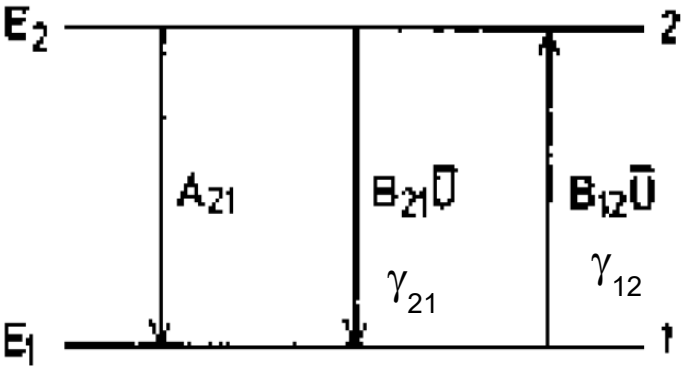

At equilibrium

$$n_1\left(\gamma_{12}+B_{12}U(T)\right)=n_2\left(A_{21}+\gamma_{21}+B_{21}U(T)\right)$$

The collision rate is given by (density times collision probability per particle(velocity distribution))

$$C_{ik}=n\,\gamma_{ik}(v)$$

$$\frac{C_{12}}{C_{21}}=\frac{n_2\gamma_{21}}{n_1\gamma_{12}}=\frac{g_2}{g_1}\,e^{-h\nu/kT_K}$$

While the energy density due to the radiation field is

$$U(T)=\frac{4\pi}{c}B(T_b)=\frac{8\pi\nu^3}{c^3}\frac{1}{e^{h\nu/kT_b}-1}$$

Spectral lines

$$\frac{n_2 g_1}{n_1 g_2} = \exp\left(\frac{-h\nu}{kT_{ex}}\right) = \exp\left(\frac{-h\nu}{kT_b}\right) \frac{A_{21} + C_{21}\exp\left(\frac{-h\nu}{kT_K}\right)\left[\exp\left(\frac{h\nu}{kT_b}\right) - 1\right]}{A_{21} + C_{21}\left[1 - \exp\left(\frac{-h\nu}{kT_b}\right)\right]}$$

$$T_{ex}, T_b, T_K \gg T_0 = \frac{h\nu}{k} \qquad T_{ex} = T_K \frac{T_b A_{21} + T_0 C_{21}}{T_K A_{21} + T_0 C_{21}}$$

If radiation dominates (low density) $C_{21} << A_{21}$ then $T_{ex} \rightarrow T_b$ and no line is observable
If collisions dominate (high density) $C_{21} >> A_{21}$ then $T_{ex} \rightarrow T_K$ and line is observable

The critical density is the density of the cloud at which the probability of emission equals the probability of collisional processes

$$n_{cr} \approx A_{21} \approx C_{21}$$

Observations in a given transition are most sensitive to gas with densities near the corresponding critical density.

Given the on-off source measurement

$$\Delta I_\nu = I_\nu(T_K) - B_\nu(T_b) = \left(1 - e^{-\tau}\right) \frac{2h\nu^3}{c^2} \left(\frac{1}{e^{h\nu/kT_K} - 1} - \frac{1}{e^{h\nu/kT_b} - 1}\right)$$

If Tk > Tb the line appears in emission
If Tk < Tb the line appears in absorption

Spectral lines position and broadening

Spectral lines are Doppler shifted if emitting cloud is moving wrt the observer.

$$1+z=\frac{\nu_{emitted}}{\nu_{observed}}$$

Variation in the line position wrt the rest frame is a measure of cosmological distances.

Spectral lines can be broadened for

$$\frac{\Delta v}{c}=\frac{\Delta \nu}{\nu}$$

- **Natural broadening**: According to the uncertainty principle the uncertainty in energy, ΔE and the lifetime, Δt, of the excited state are related by ΔE/Δt>h/2 This determines the minimum possible line width.

- **Doppler broadening**: due to intrinsic motions of (parts of) the cloud wrt the observer The higher the temperature of the cloud, the wider the distribution of velocities in the cloud Hence the emission is characterized by a velocity distributions that is described by the shape of the spectral lines with frequency A(ν). If this were the only effect the line shape would be Gaussian

- **Pressure broadening** (Collision broadening). Collisions between atoms or molecules reduce the lifetime of the upper state, Δt, increasing the uncertainty ΔE.

Spectral lines shape

The line shape is a function of the frequency and hence of the velocity A(ν)

$$M_0 = \Delta\nu \sum_\nu A(\nu)$$

The **zeroth momentum** of the distribution is the integrated flux density

The **first momentum** of the distribution is the intensity-weighted velocity of the spectral line and hence a measure for the mean velocity of the gas.

$$M_1 = \frac{\sum_\nu \nu A(\nu)}{\sum_\nu A(\nu)}$$

The **second momentum** is a measure for the velocity dispersion, σ, of the gas along the line of sight, i.e. the width of the spectral line

$$M_2 = \sqrt{\frac{\sum_\nu (\nu - M_1)^2 A(\nu)}{\sum_\nu A(\nu)}}$$

By mapping the sources in different frequency channels, allows to reconstruct the spatial distribution of the velocity field

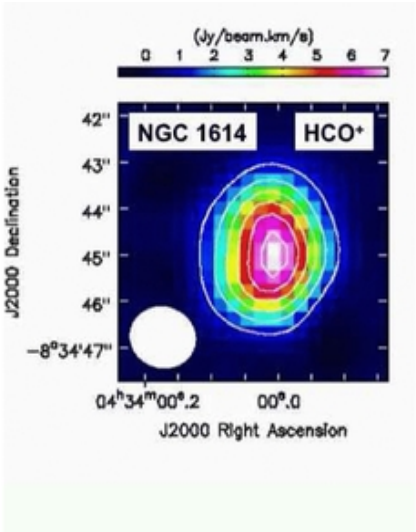

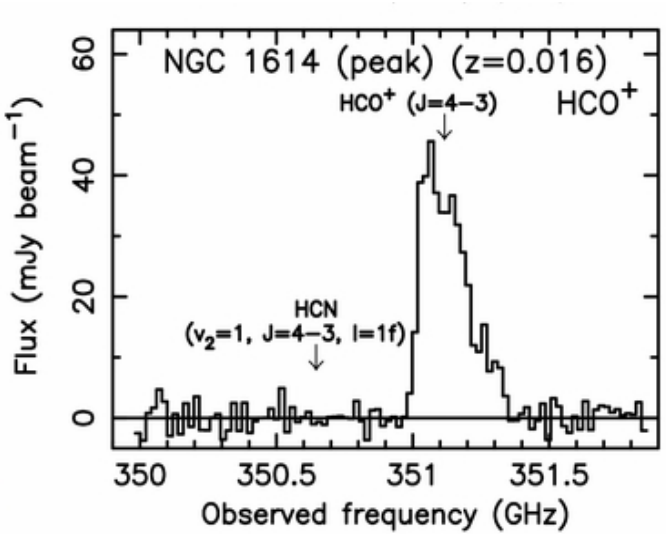

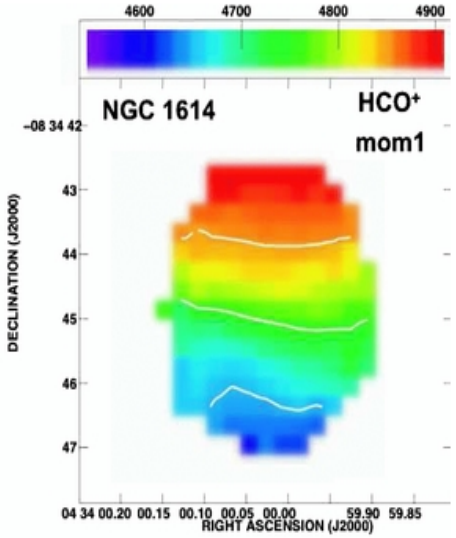

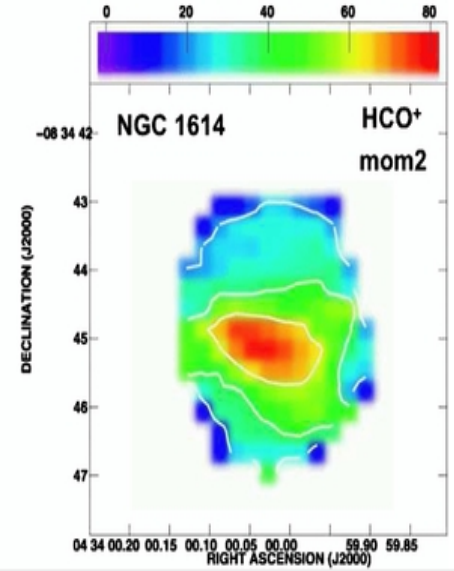

(ALMA HCO+ In NGC 1614
Imanishi et al. 2013)

Line signatures

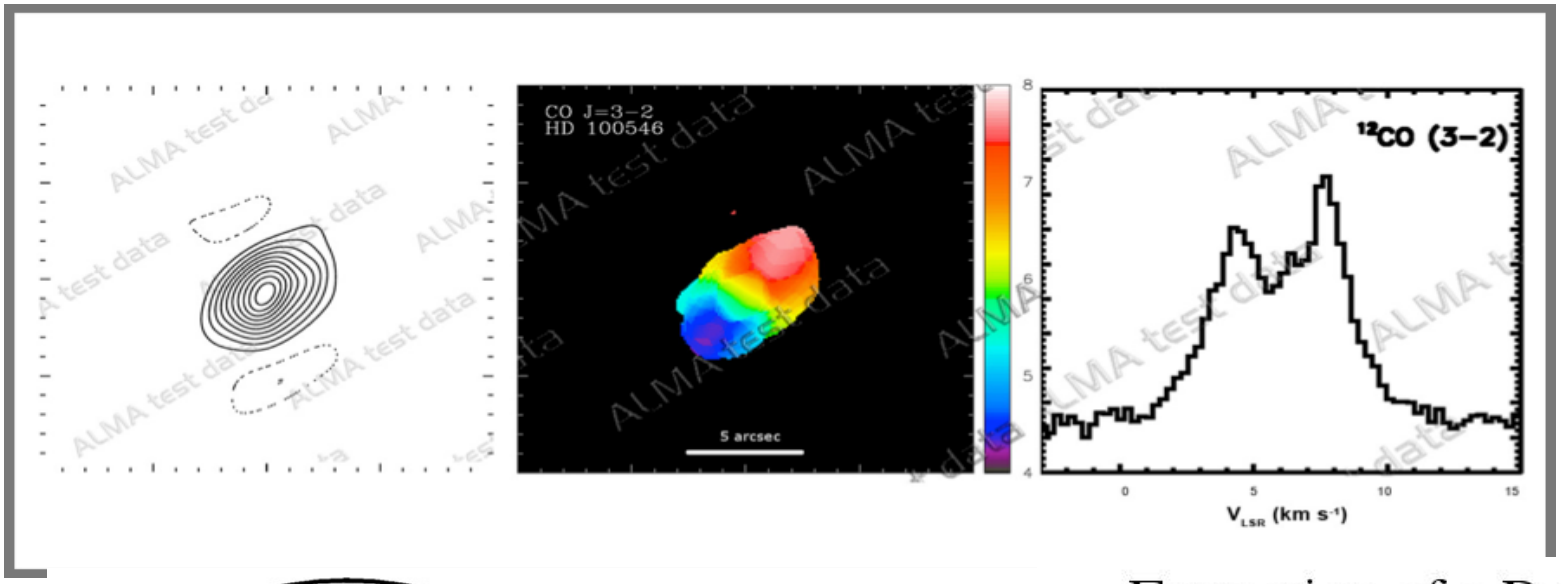

Rotating disk

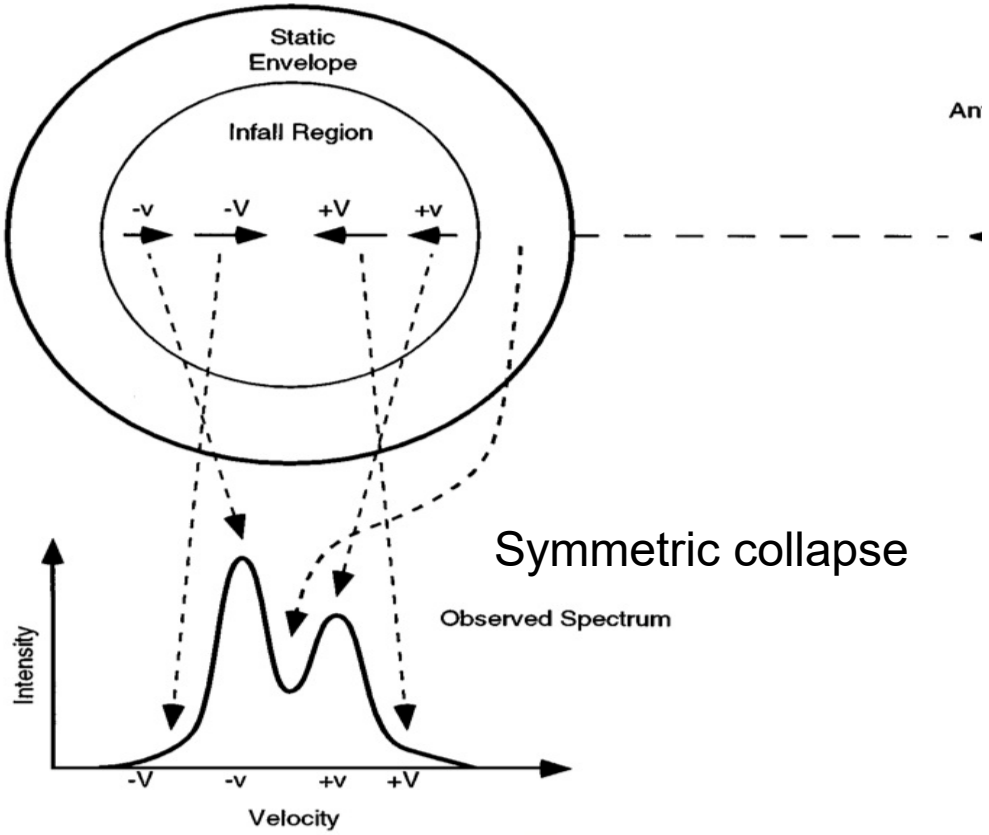

Symmetric collapse

Formation of a P-Cygni Line- Profile

(Symmetric expansion)

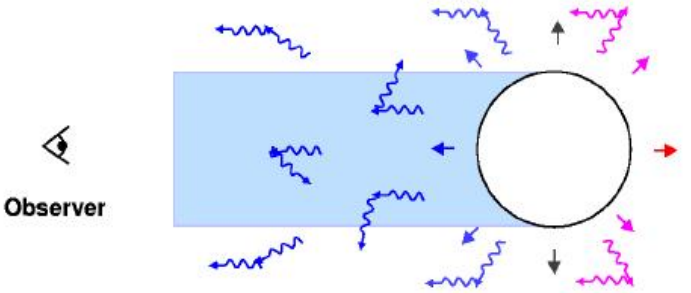

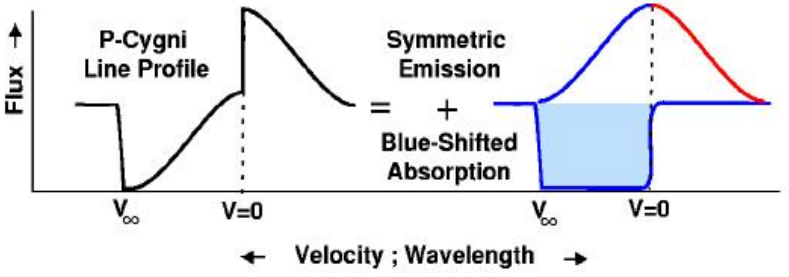

Atomic lines

Atomic transitions at sub(mm) wavelengths mostly arise from spin-orbit interactions:
by changing the spin direction, the electron jumps from a fine structure level to another, because of an electromagnetic interaction between the electron's spin and the magnetic field generated by the electron's orbit around the nucleus.

In molecular clouds such transitions can be collisionally stimulated.

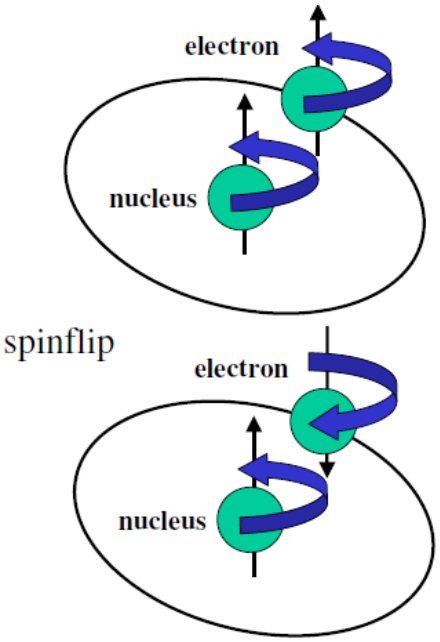

J is the total angular momentum number so that J=L±S with L=0,...,n-1

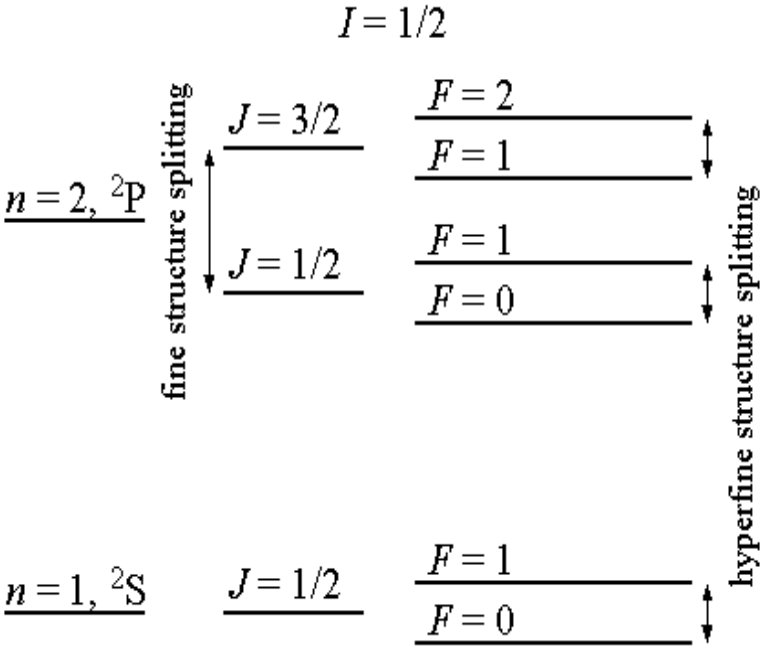

Atomic lines

Element and ionization state	Transition	ν/GHz	A_{ij}/s^{-1}	Critical density n^*	Notes
CI	$^3P_1 - ^3P_0$	492.16	7.93×10^{-8}	5×10^2	b
CI	$^3P_2 - ^3P_1$	809.34	2.65×10^{-7}	10^4	b
CII	$^2P_{3/2} - ^2P_{1/2}$	1900.54	2.4×10^{-6}	5×10^3	b
OI	$^3P_0 - ^3P_1$	2060.07	1.7×10^{-5}	$\sim 4 \times 10^5$	b
OI	$^3P_1 - ^3P_2$	4744.77	8.95×10^{-5}	$\sim 3 \times 10^6$	a,b
OIII	$^3P_1 - ^3P_0$	3392.66	2.6×10^{-5}	$\sim 5 \times 10^2$	a
OIII	$^3P_2 - ^3P_1$	5785.82	9.8×10^{-5}	$\sim 4 \times 10^3$	a
NII	$^3P_1 - ^3P_0$	1473.2	2.1×10^{-6}	$\sim 5 \times 10^1$	a
NII	$^3P_2 - ^3P_1$	2459.4	7.5×10^{-6}	$\sim 3 \times 10^2$	a
NIII	$^2P_{3/2} - ^2P_{1/2}$	5230.43	4.8×10^{-5}	$\sim 3 \times 10^3$	a,b

[a] ions or electrons as collision partners
[b] H_2 as a collision partner

In cold regions, cooling is dominated by collisional excitation of C+
by collisions with thermal electrons followed by emission of infrared fine-structure lines.
As the temperature rises, other species begin to contribute collisionally excited lines to the cooling

CII

The ground state of C+ has a fine-structure transition with excitation energy (in temperature units) of 92 K, which emits a far-infrared photon with a wavelength of 158μm.

The [CII] line traces photodissociation regions (PDRs) as well as diffuse HI and HII regions. It should be an excellent tracer of the global galactic star formation activity, including that of somewhat lower-mass (A+B) stars (Stacey et al 1991).

The line emission contains between 0.1 and 1% of the bolometric luminosity of any galaxy.

In local galaxies, the [CII] line is proportional to total far-IR flux.
-3<log(L_CII/Lfir)<-2 in local LIRG.
There is a trend for AGNs to have lower L_CII/Lfir ratios than SMGs (because of stronger UV fields, higher opacity).
The ratio is an order of magnitude higher at higher z for objects of the same luminosity (lower dust content = lower metallicities and more efficient cooling, Maiolino et al. 2009).
Hence cooling is more effective at high-z as observed in local galaxies with low metallicity.

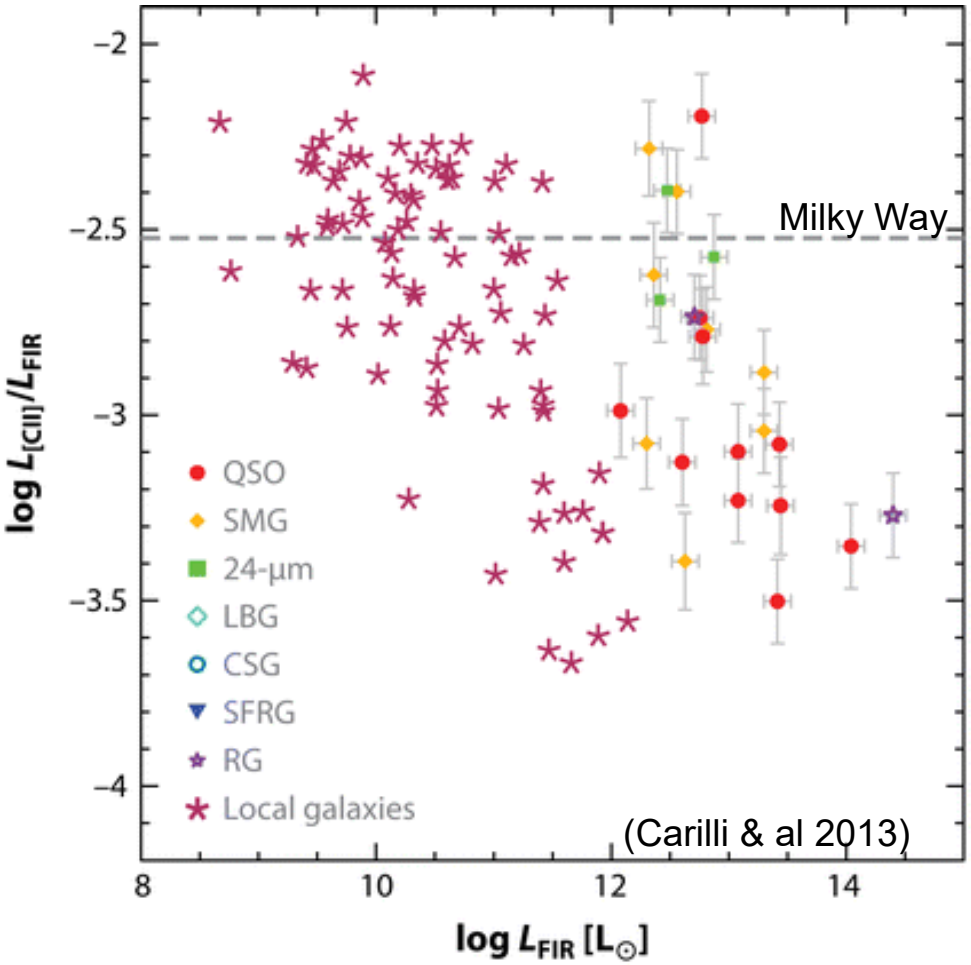

Molecular lines

Molecular transitions according to different energies, W :

a) electronic transitions with typical energies of a few eV – that is lines in the visual or UV regions of the spectrum;

b) vibrational transitions caused by oscillations of the relative positions of atoms with respect to their equilibrium positions. Typical energies are 0. 1− 0. 01 eV, corresponding to lines in the infrared region of the spectrum;

c) **rotational transitions caused by the rotation of the atoms with typical energies of ~= 10−3 eV corresponding to lines in the cm and mm wavelength range.**

$$W^{\text{tot}} = W^{\text{el}} + W^{\text{vib}} + W^{\text{rot}}$$

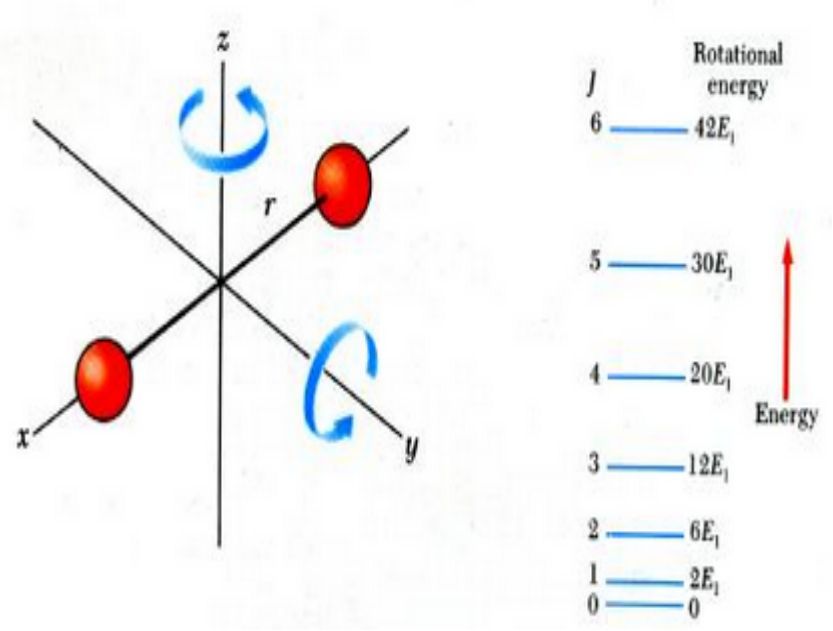

J is the molecular orbital angular momentum number corresponding to the angular momentum perpendicular to the line connecting the nuclei

$$L = I\omega = \left(\frac{m_A m_B}{m_A + m_B}\right) r_e^2 \omega = m r_e^2 \omega \qquad E_{\text{rot}} = \frac{I\omega^2}{2} = \frac{L^2}{2I} = \frac{J(J+1)\hbar^2}{2I}$$

the quantum of energy associated with a transition from J to J-1 is

$$\Delta E_{\text{rot}} = [J(J+1) - (J-1)J]\frac{\hbar^2}{2I} = \frac{\hbar^2 J}{I}$$

(I is the inertia momentum). That corresponds to a ladder at frequencies

$$\nu = \frac{\Delta E_{\text{rot}}}{h} = \frac{\hbar J}{2\pi I} = \frac{hJ}{4\pi^2 m r_e^2}, \qquad J = 1,\ 2, \ldots$$

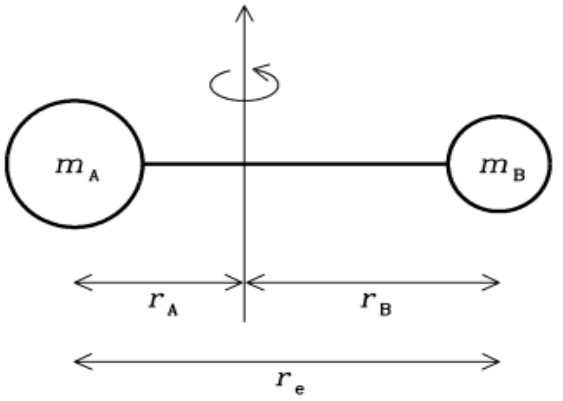

CO vs H2

H2 is the most abundant molecula tracing the molecular mass in clouds and plays a key role in excitation, thermal balance, and gas-phase chemistry, but it is a homonuclear linear molecule

- it has no permanent dipole moment
  - -> can be vibrationally excited at high temperatures, observable in MIR, but the warm molecular gas at these temperatures (100-1000K) is only a small fraction (~5%) of the cool molecular gas (Roussel et al. 2007
  - -> dipole rotational transitions have low probability and require high excitation energies (only quadrupole rotational transitions are allowed but very weak)

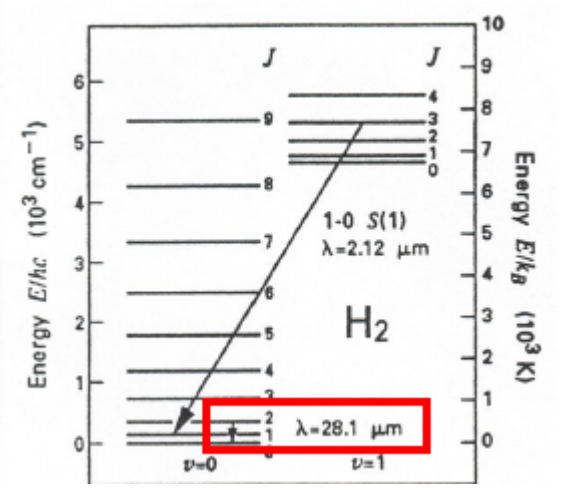

-the excited levels are at high T so under normal interstellar conditions these are not populated except in regions of high excitation (e.g., shocks).

CO is the second most abundant molecula in molecular clouds

- rotational transitions are allowed with critical density ~10^3 cm^{-3} quite common in molecular clouds
- its formation is catalyzed by H2 via $H2+C^+ \rightarrow CH + CH2$, $CH+O2 \rightarrow CO+H2$
- rotational transitions are excited by collisions with H2
- J(1-0) transition is at 115.27 GHz
- as it is optically thick its luminosity is a measure of the surface density and allows to estimate virial masses.

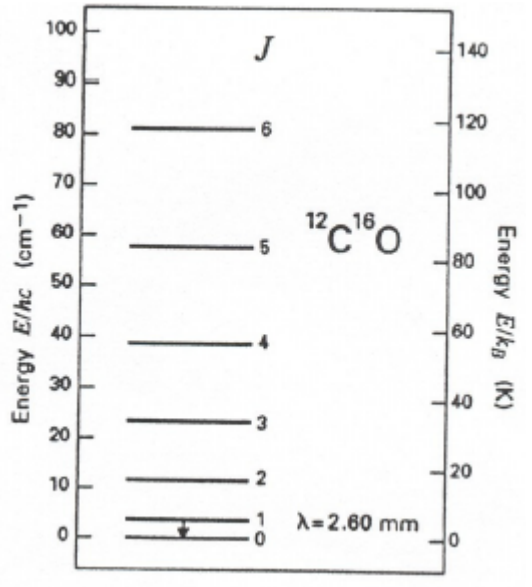

CO vs H2

$$L_{CO} = D^2 \int I_{CO}\, d\Omega = T_A^*(CO)\Delta v \pi R_C^2 = \left(\frac{3\pi G}{4\rho_C}\right)^{1/2} T_A^*(CO) M_C$$

$$I_{CO} = \int T_A^* dv \qquad \Delta v = \left(\frac{GM_C}{R_C}\right)^{1/2} \qquad \rho_C = \frac{3M_C}{4\pi R_C^3}$$

$$M(\mathrm{H_2}) = \alpha L'_{\mathrm{CO}}$$

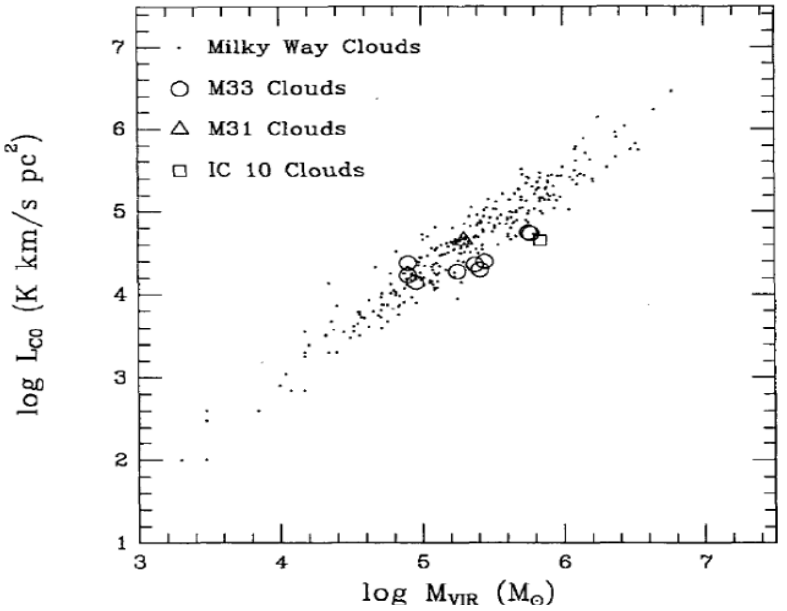

Indeed, the precise value of the conversion factor depends on the density, temperature and metallicity of the gas

$\alpha \equiv M_{\mathrm{gas}}/L'_{\mathrm{CO}} = 4.6\ M_\odot\ (\mathrm{K\ km\ s^{-1}\ pc^2})^{-1}$ in MW type galaxies (with increase in low metallicity)

$\alpha \sim 0.8\ M_\odot\ (\mathrm{K\ km\ s^{-1}\ pc^2})^{-1}$ in SMGs and quasar hosts

The difference is due to the fact that CO does not arise in virialized molecular cloud, but also in the warm PDR. Hence **the line emission is due to the total dynamical mass.**
The different values are consistent with a more extended disk-like CO distribution and lower CO excitation in MW type galaxies, compared to more compact morphologies, higher excitation in SMG and QSO.

The star formation law

The star formation law describes how efficiently galaxies turn their gas into stars.
The volume density of star formation is a function of the gas surface density

$$\Sigma_{\rm SFR} = A\ \Sigma_{\rm gas}^{N}$$

According to Kennicutt (1998) N=1.4 (determined empirically).

Measurement of surface densities requires resolved observations of galaxies.
The gas density is almost completely due to H2.
Hence, CO is a tracer of the gas surface density
(with all the caveats on the CO vs H2 mass determination)

The SFR is traced by the integrated IR luminosity

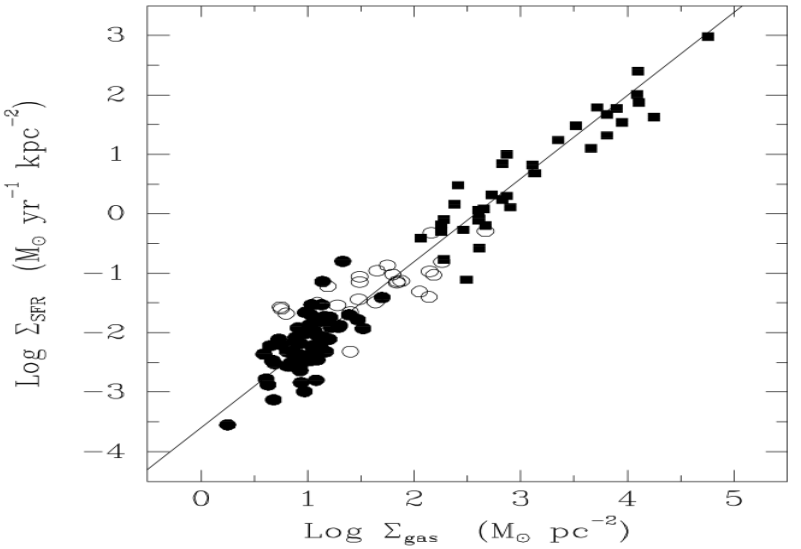

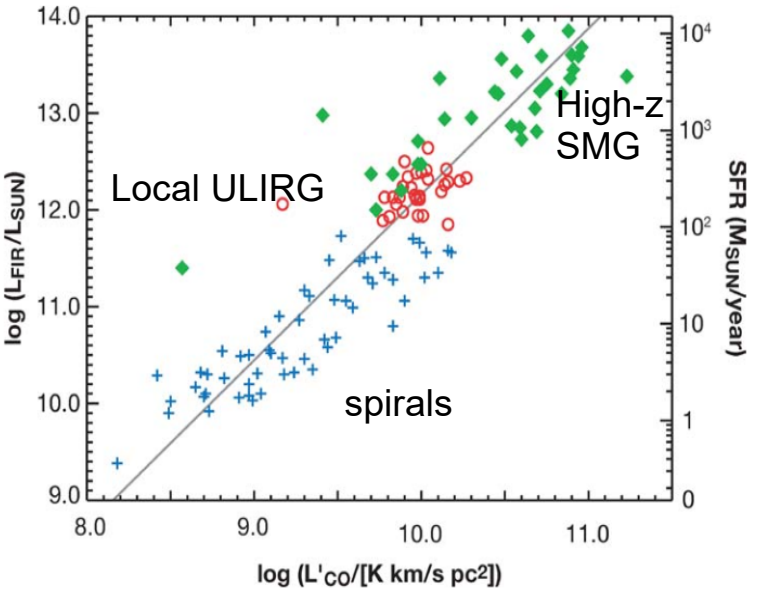

The star formation law

High-z observations suffer of low resolution and so far exploited high-J CO transitions
Including high-z there are two trends:

For starbursts $\log(L_{\rm IR}) = 1.37(\pm0.04) \times (\log L'_{\rm CO}) - 1.74(\pm0.40)$

For MW type galaxies $\log(L_{\rm IR}) = 1.13 \times (\log L'_{\rm CO}) + 0.53$

The gap arises from similar arguments as for the L_CO-H2 mass relation
Also the time of gas comsumption depends on the α coefficient.

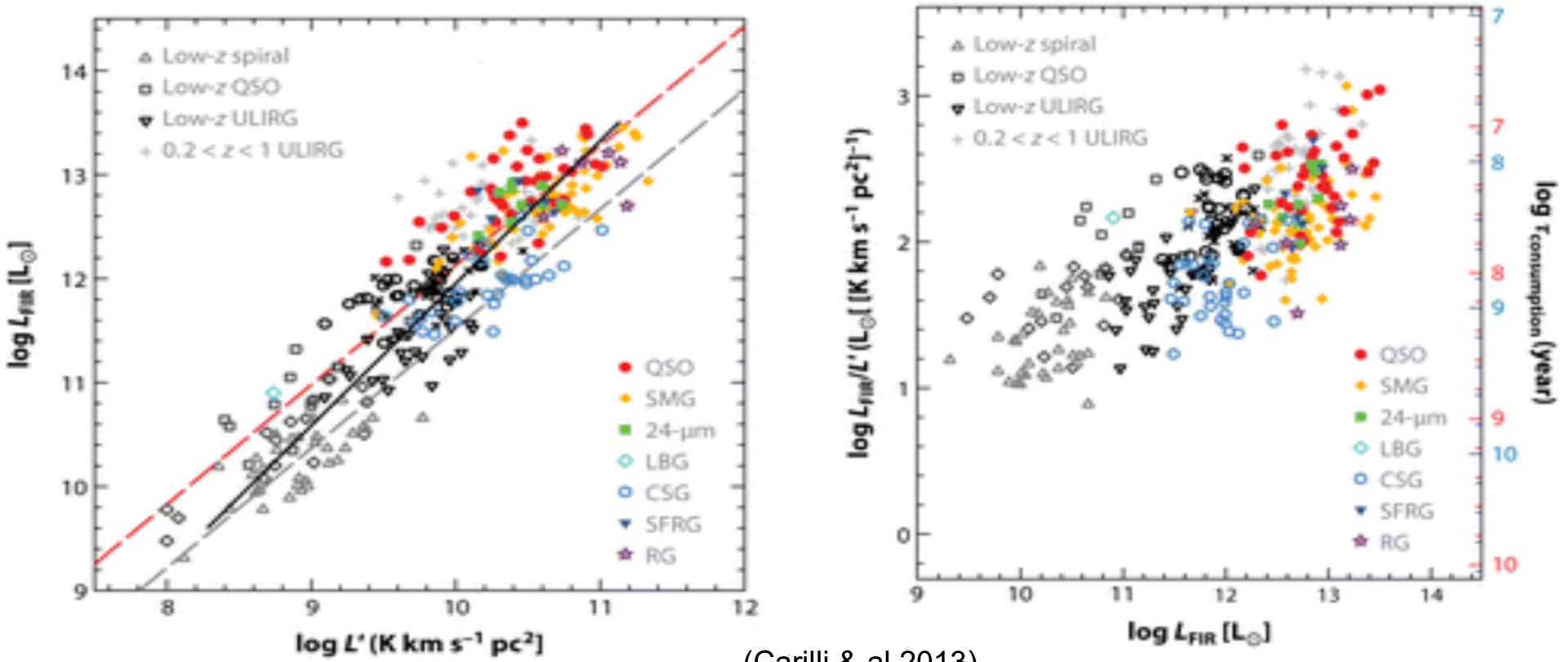

(Carilli & al 2013)

PDRs

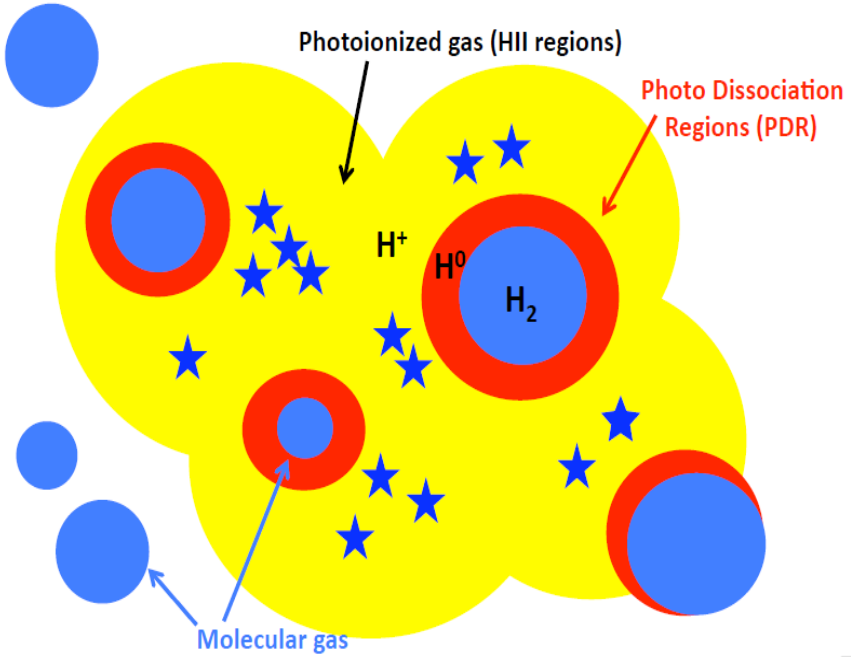

Photo-Dissociation Regions (PDR=photon-dominated regions) are the warm, partially ionized surfaces between the region where UV radiation from stars ionizes the gas and the cold molecular clouds. In these regions H2 is dissociated in HI. These regions are also rich of dust. Excitation From UV radiation together with low density make PDR the origin of spectral lines in FIR and sub-mm

The dominant species are H, C, O and N.

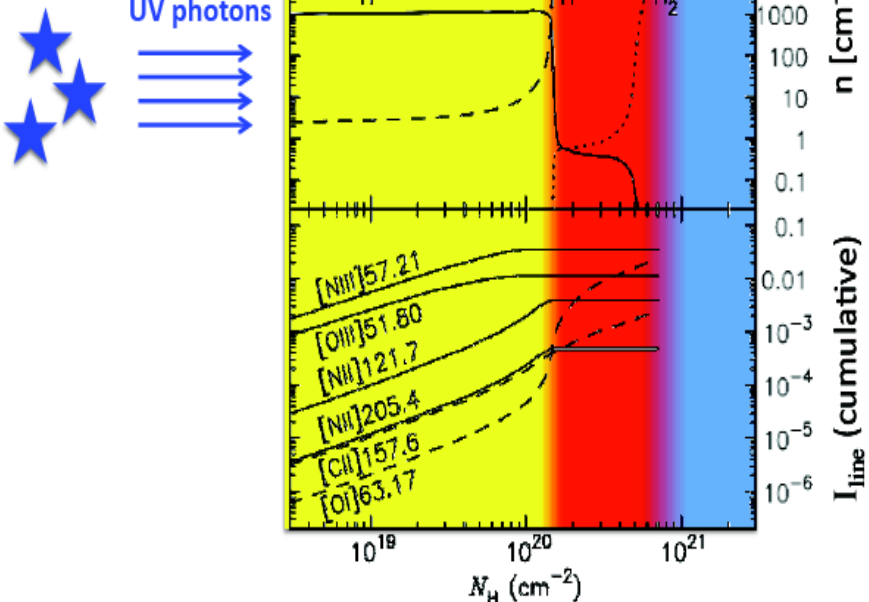

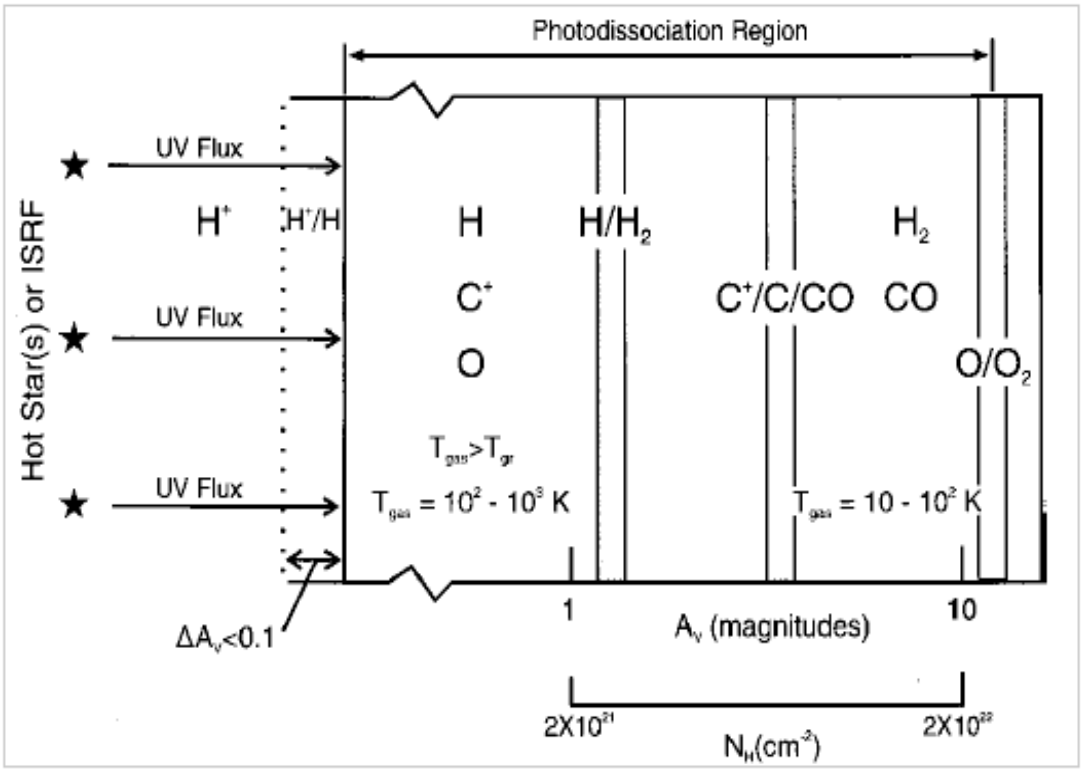

XDRs

X-rays have a larger penetration depth than UV-photons.

Hence in presence of X-ray sources molecular clouds can be penetrated by radiation and get higher temperature and emissions are different than in PDRs. The regions surrounding X-ray sources are referred as X-ray dominated regions. X-ray sources that are relatively closer to us are young stellar objects (YSO) with protoplanetary disks, and the associated X-ray spectra can form XDRs in some parts of the disks. XDRs are also seen in active galactic nuclei (AGNs) in other galaxies.

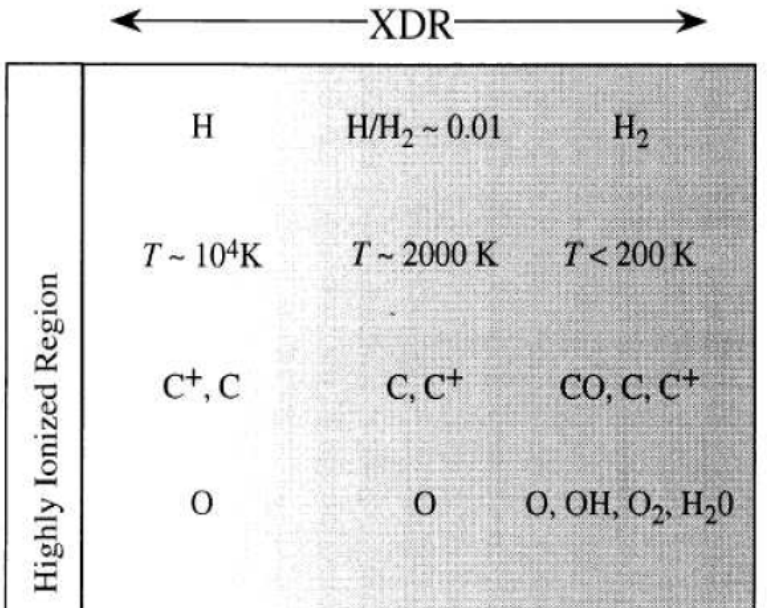

Presence of XDR species is a discriminant of AGN activity vs starburst activity.

In XDR there are enhancement of CN and HCN because of high ionization.
This leads to higher ratios of HCN/CO and CN/HCN.

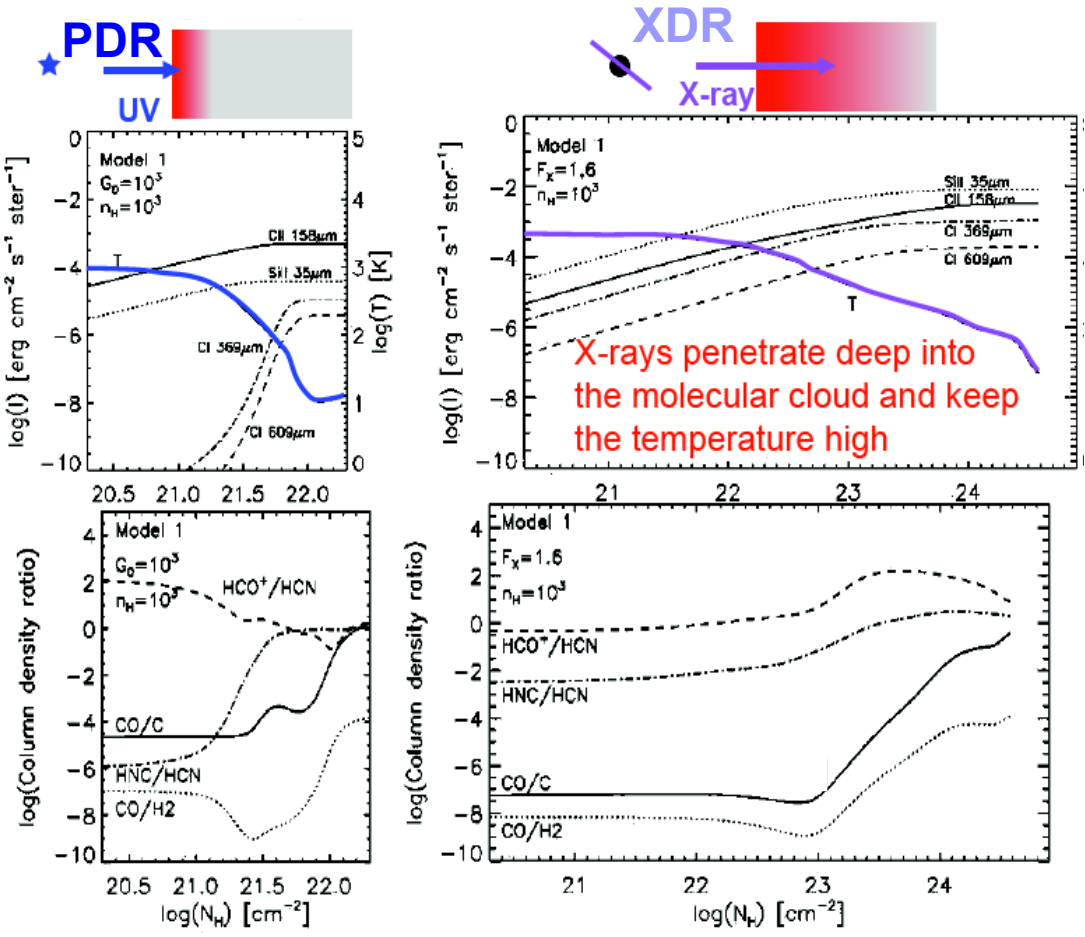

HCN & HCO+

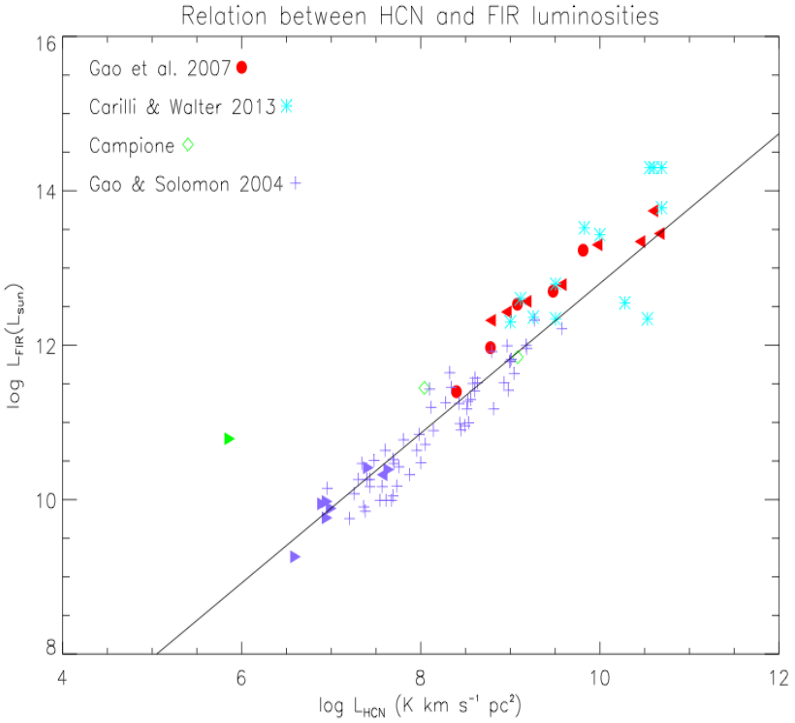

A linear relation links also Lfir and HCN.

$$logL_{IR} = 1.00(\pm 0.05)\, logL_{HCN} + 2.9$$

Only few observations are available so far at high-z (HCN is 10 times fainter than CO), but there are indications of lower L_HCN than predicted from low-z extrapolations, maybe on the effect of denser environment at high-z and/or higher SF efficiency.

HCN is enhanced in XDR wrt CO and HCO+, so it can discriminate AGN and starforming galaxies.

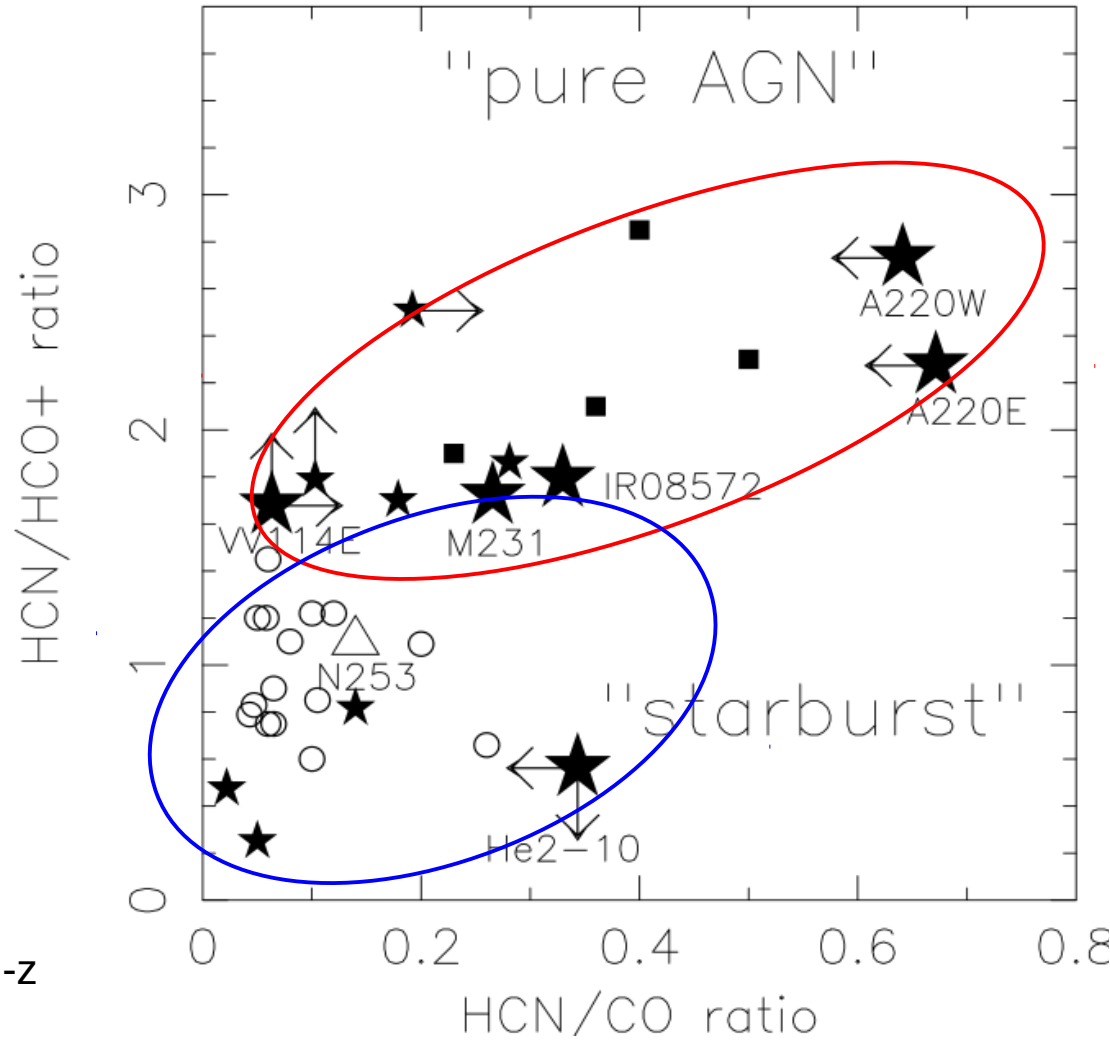

(Gao et al. 2007, Khono et al. 2005
Courtesy by E. Bianchi)

HCN in XDR

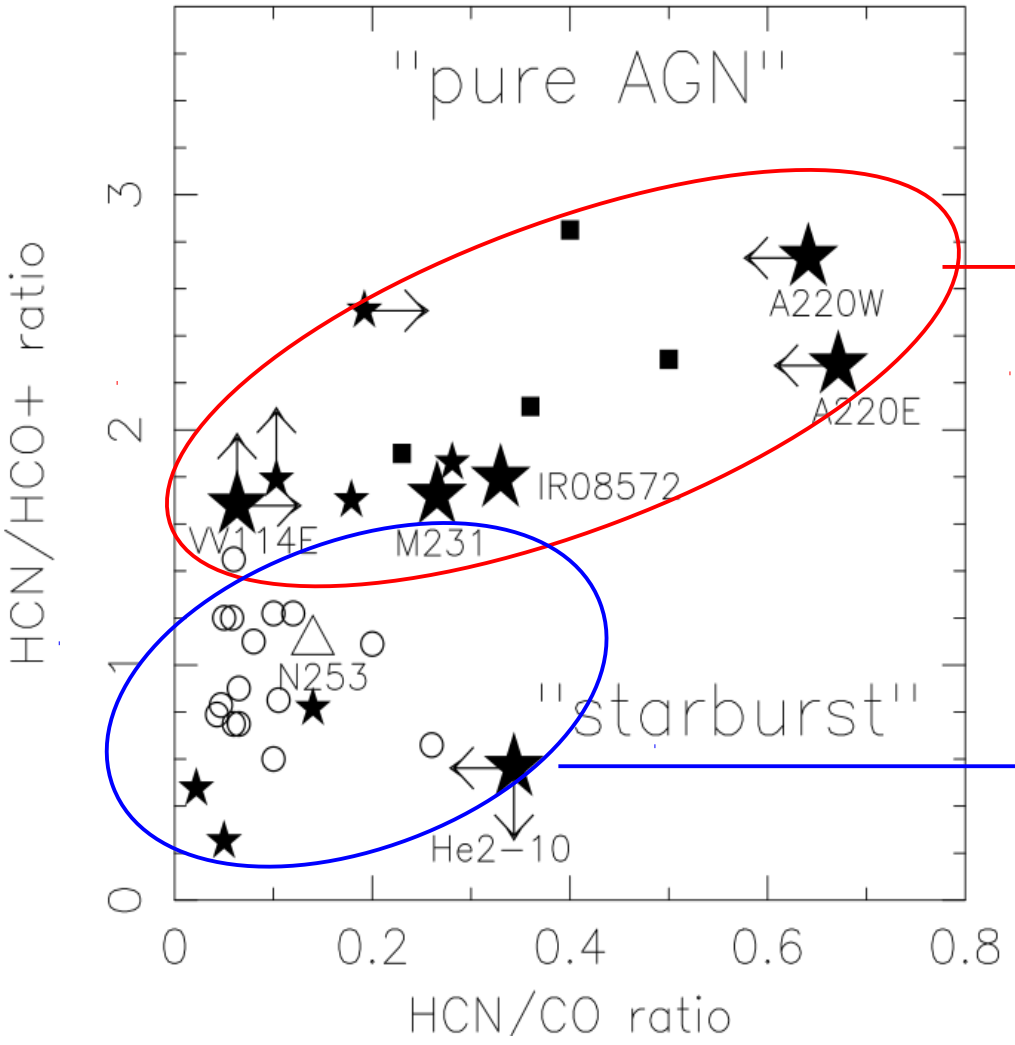

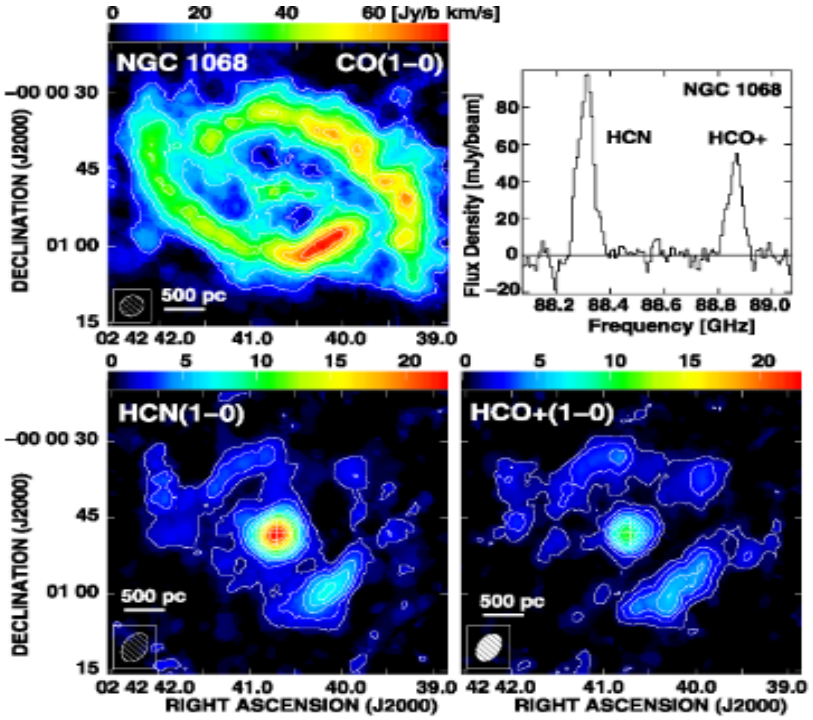

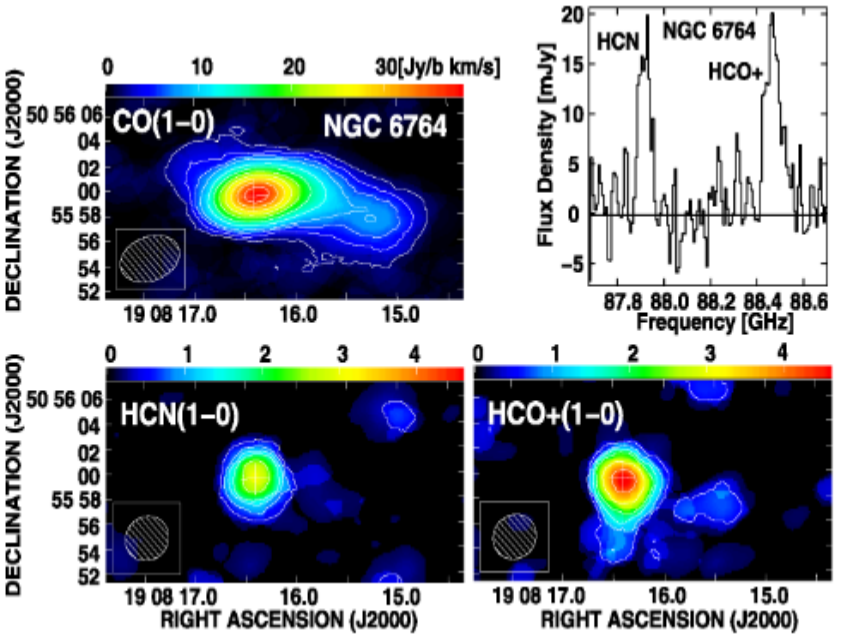

(Khono et al. 2008, Imanishi et al. 2007)

Intensity ratios

Ratios of intensity of different lines are tracer of physical conditions in the clouds
In molecular clouds they are used to derive T, tau, density. E.g. by taking the ratio between same transition of different isotopes of same molecule, or between different transitions of same isotope.
In particular help to distinguish PDR from XDR:

- **PDR intensities depend on surface density, while on column density in XDR.**
- Fine structure emissions are produced on the edge of the cloud, while in the XDR all the cloud contributes.
- Thin lines (CII) are stronger in PDR (because of lower recombination probability), thick lines (CO) are stronger in XDR (because consider all the volume)

- Higher J transition have higher critical densities, so ratios between very different J levels help distinguishing PDR and XDR.
  SLEDs allow to distinguish the emitting regions and the properties of the populations.

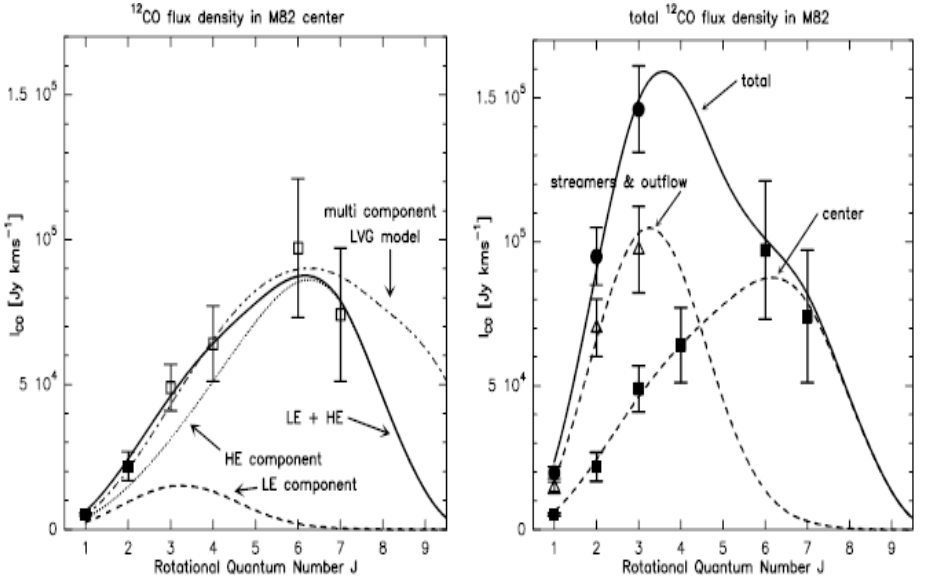

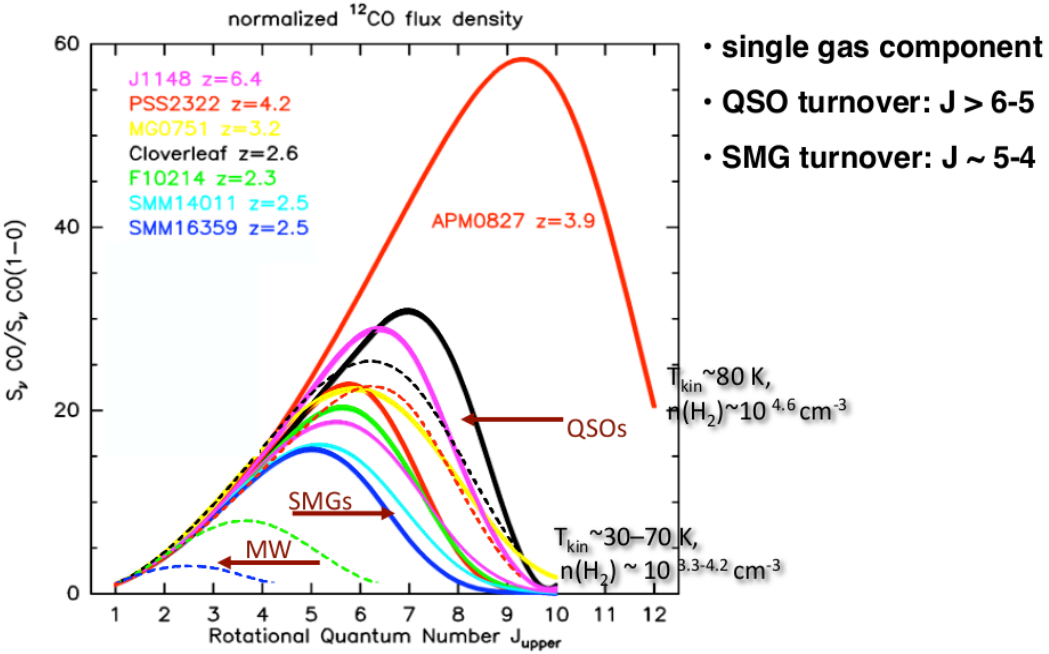

Astrochemistry

About 150 different molecules have been detected.

Most interstellar and circumstellar molecules are organic in nature (i.e. dominated by C).
Of the detected species with >6 atoms (ca. 50), 100% are organic even.
Species with >6 atoms are called complex organic molecules (COMs) (Herbst et al. 2009).

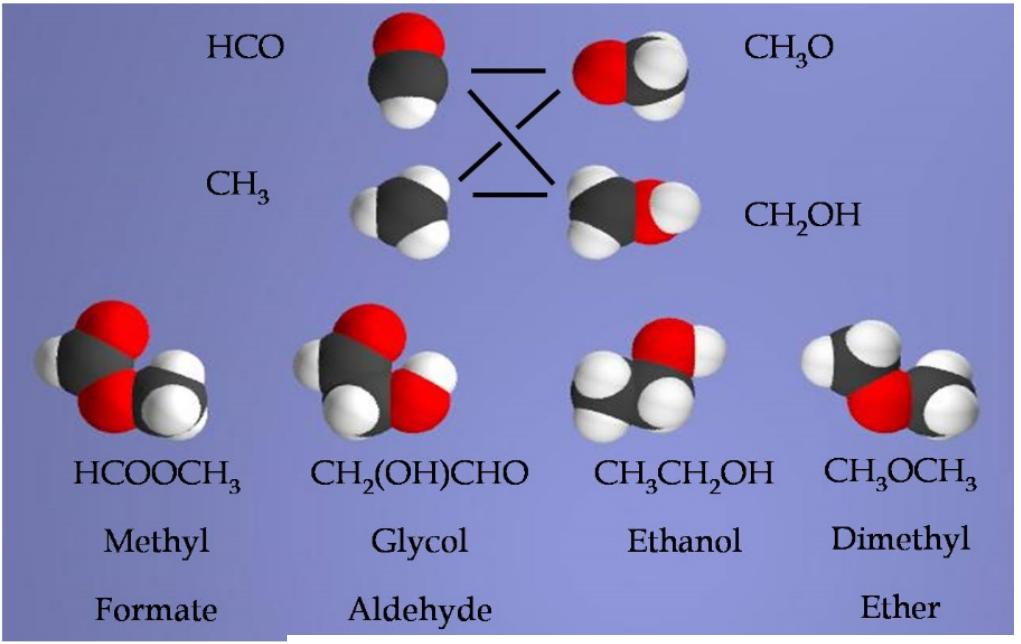

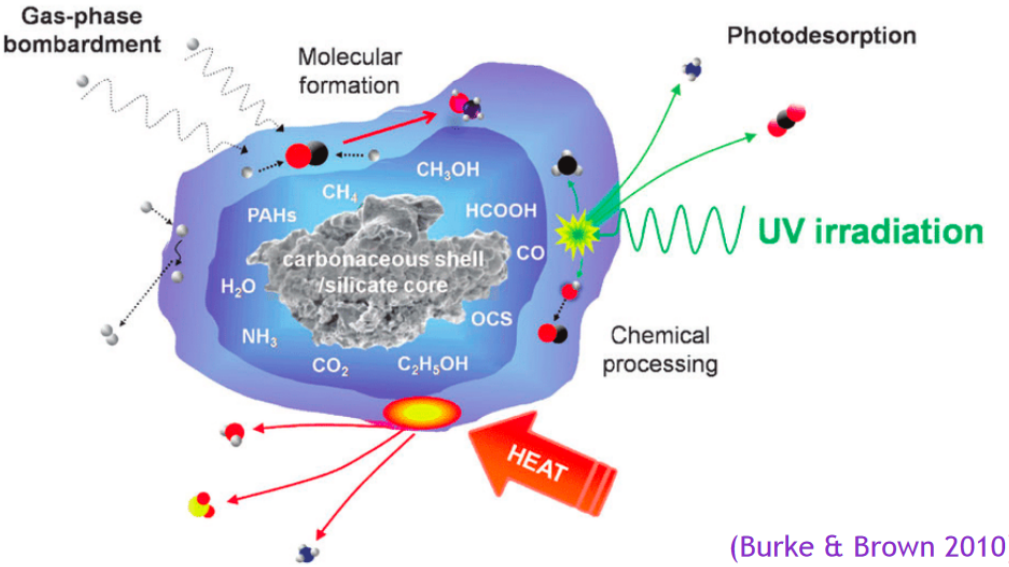

(Burke & Brown 2010)

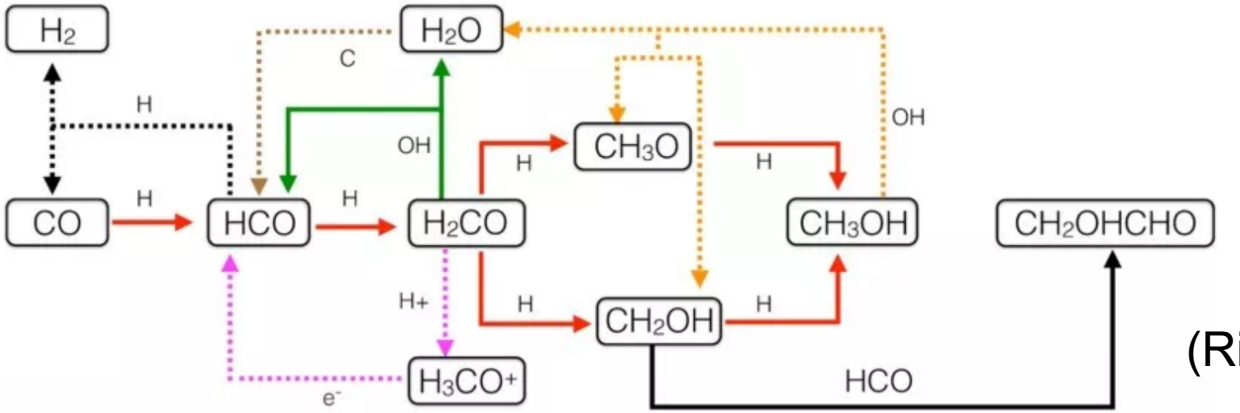

(Rivilla et al. 2018)

Astrochemistry

About 150 different molecules have been detected.

Most interstellar and circumstellar molecules are organic in nature (i.e. dominated by C).
Of the detected species with >6 atoms (ca. 50), 100% are organic even.
Species with >6 atoms are called complex organic molecules (COMs) (Herbst et al. 2009).

COMs have been found basically everywhere
(circumstellar envelopes, outflows, hot/cold/lukewarm cores, etc.)
and different types of sources can be associated with different types of COMs.
Relative abundances and presence of derived species (isophotologue, deuterated, vibrationally excited...) are used to constrain pathways to molecules formation.

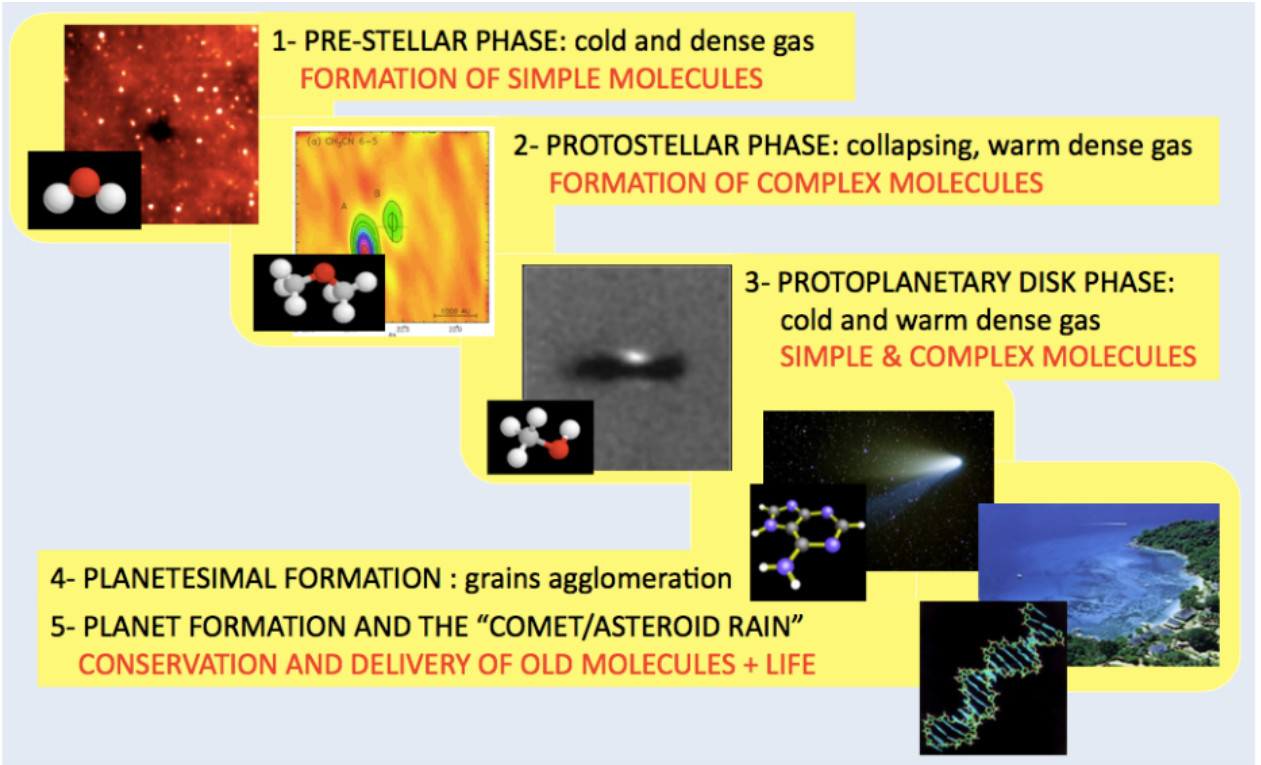

Caselli & Ceccarelli (2012)

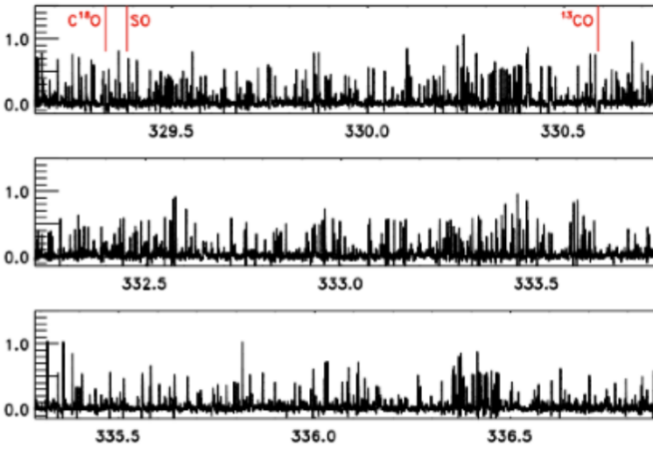

Shock chemistry

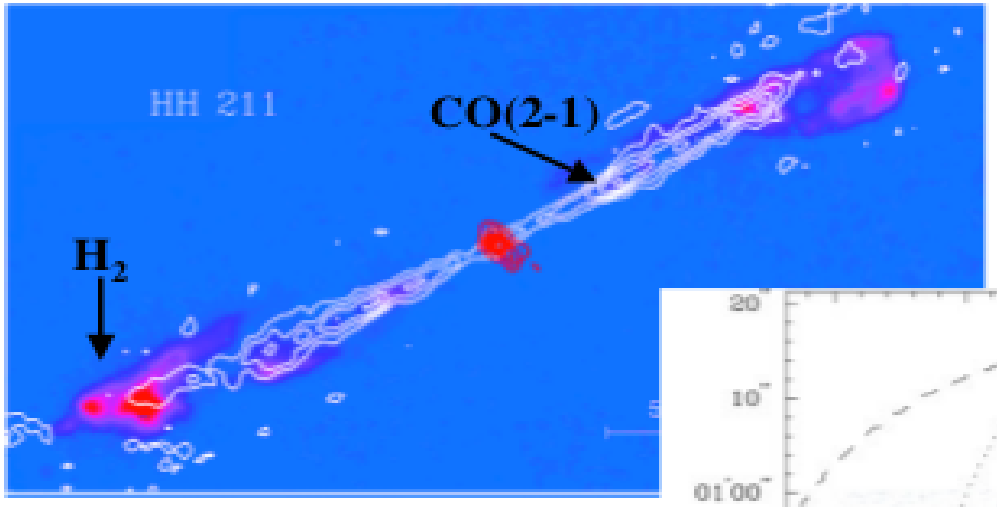

Gueth & Guilloteau (1999)

HH211

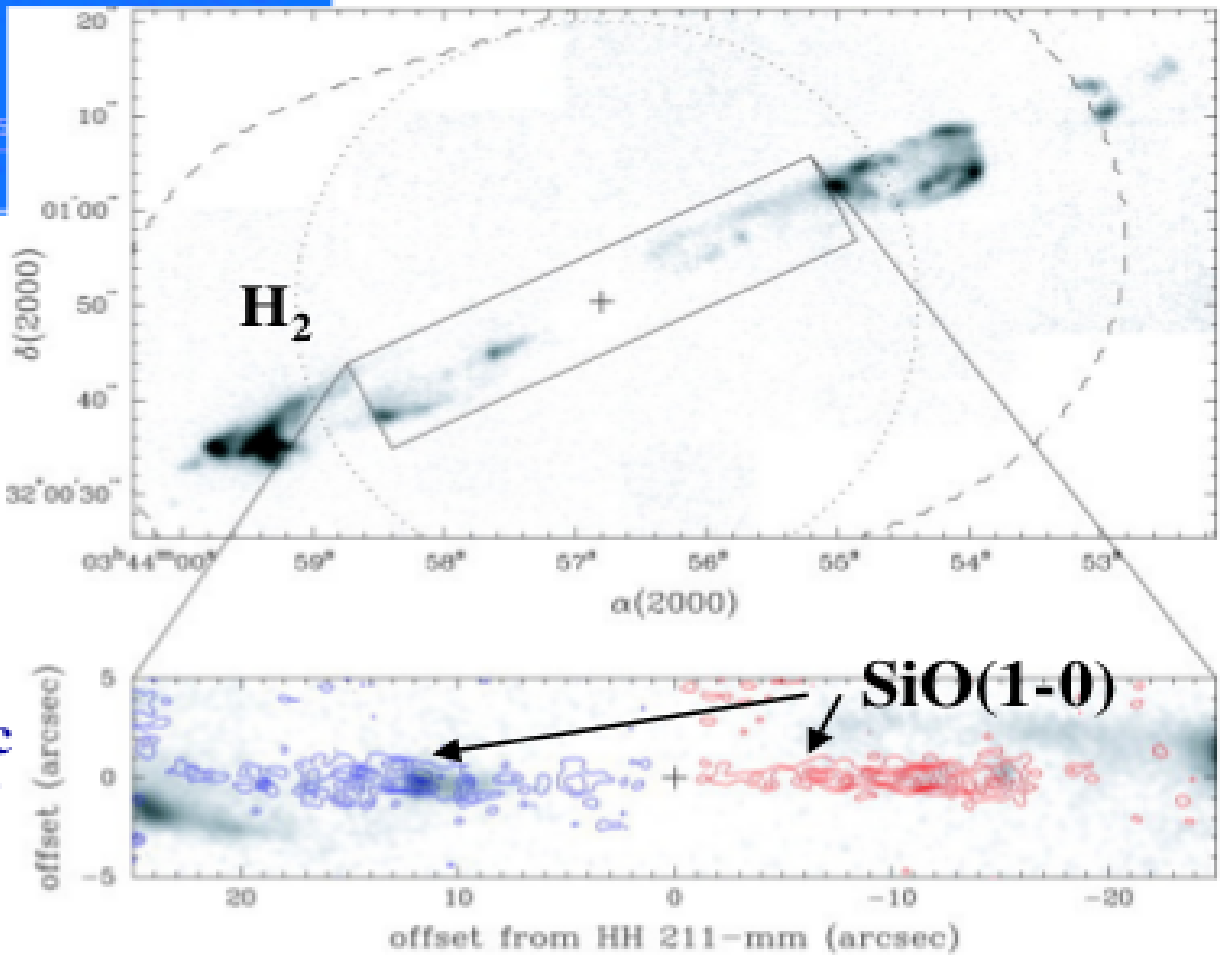

Chandler & Richer (2001)

The heating and compression caused by shocks gives rise to dramatic effects in the chemical composition of the surrounding cloud.

Dissociation, endothermic reactions, sublimation of ices and disruption of grains lead to a shock-chemistry

Shock chemistry

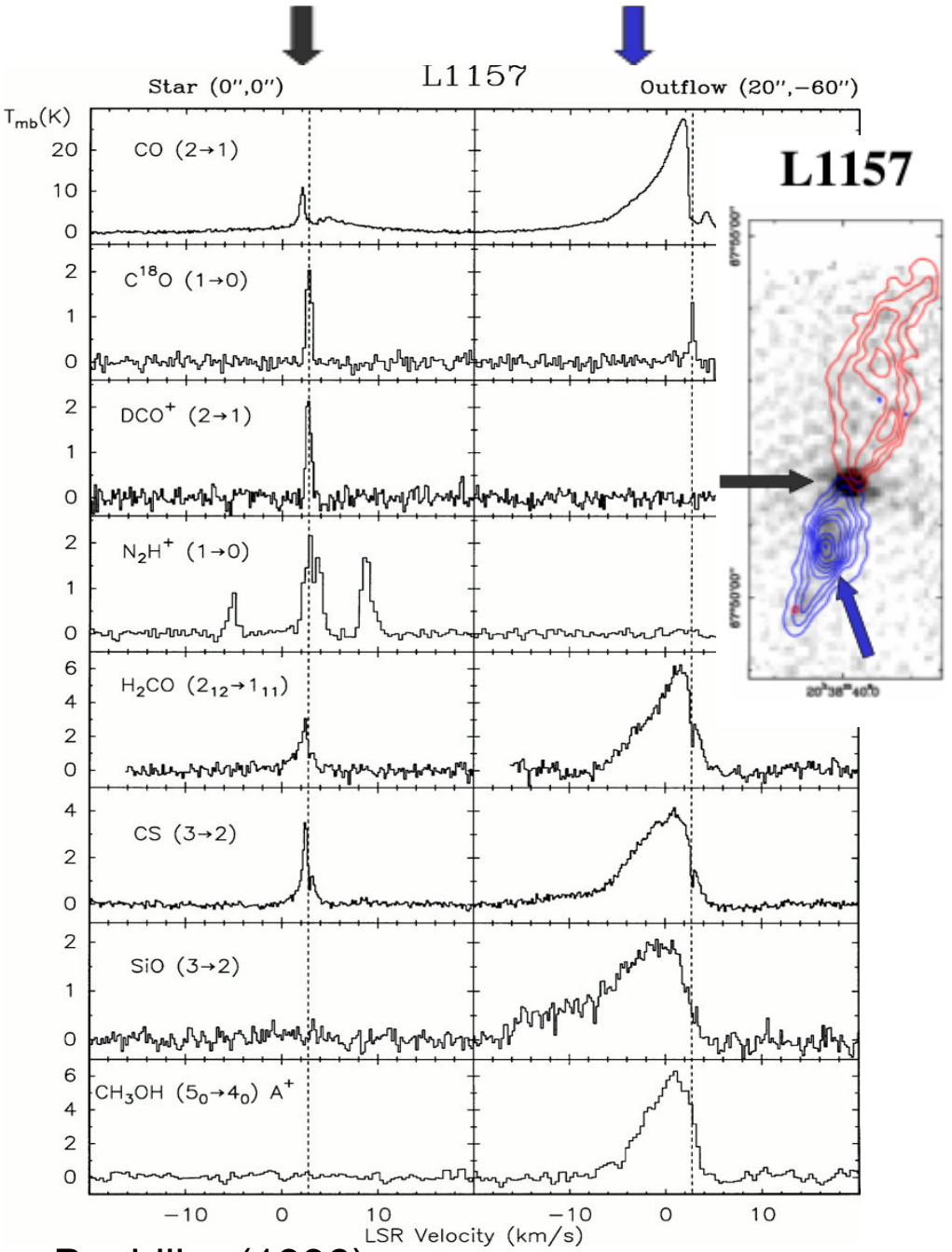

Bachiller (1996)

A mm-line survey toward the L1157 outflow.
The narrow line profiles arise from cold quiescent gas,
Toward the bow shock region the profiles are dominated by the broad lines associated with the shock.
DCO+ and N2H+ are only observed toward the cold gas condensation around the exciting source
SiO and methanol (CH3OH) only trace the hot warm gas in the shock.
CS and H2CO lines are in both gas components.

The emission of shock-chemistry molecules is seen at the position of the bowshocks, but SiO emission is also seen arising from shocks along the highly collimated molecular outflow.
It seems clear that SiO is a result of the shock chemistry following the destruction of the refractory grain cores.

Other molecules such as ammonia and methanol, which are known to be abundant in the ice dust mantles, could be directly desorbed from them. Deuterated species could also be removed from the grains by grain-grain collisions. The origin of other molecules such as SO and HCO+ is even less clear.

Molecules in the ISM or circumstellar shells (07/2018; Koln list)

2 atoms	3 atoms	4 atoms	5 atoms	6 atoms	7 atoms	8 atoms	9 atoms	10 atoms	11 atoms	12 atoms	>12 atoms
H_2	C_3 *	*c*-C_3H	C_5 *	C_5H	C_6H	CH_3C_3N	CH_3C_4H	CH_3C_5N	HC_9N	*c*-C_6H_6 *	C_{60} *
AlF	C_2H	*l*-C_3H	C_4H	*l*-H_2C_4	CH_2CHCN	$HC(O)OCH_3$	CH_3CH_2CN	$(CH_3)_2CO$	CH_3C_6H	*n*-C_3H_7CN	C_{70} *
AlCl	C_2O	C_3N	C_4Si	C_2H_4*	CH_3C_2H	CH_3COOH	$(CH_3)_2O$	$(CH_2OH)_2$	C_2H_5OCHO	*i*-C_3H_7CN	C_{60}^+ *
C_2**	C_2S	C_3O	*l*-C_3H_2	CH_3CN	HC_5N	C_7H	CH_3CH_2OH	CH_3CH_2CHO	$CH_3OC(O)CH_3$	$C_2H_5OCH_3$?	*c*-C_6H_5CN 2018
CH	CH_2	C_3S	*c*-C_3H_2	CH_3NC	CH_3CHO	C_6H_2	HC_7N	CH_3CHCH_2O 2016			
CH^+	HCN	C_2H_2*	H_2CCN	CH_3OH	CH_3NH_2	CH_2OHCHO	C_8H	CH_3OCH_2OH 2017	SO^+	SO_2	HCNO	NH_4^+
CN	HCO	NH_3	CH_4 *	CH_3SH	*c*-C_2H_4O	*l*-HC_6H *	$CH_3C(O)NH_2$		SiN	*c*-SiC_2	HOCN	H_2NCO^+
CO	HCO^+	HCCN	HC_3N	HC_3NH^+	H_2CCHOH	CH_2CHCHO (?)	C_8H^-		SiO	CO_2 *	HSCN	$NCCNH^+$
CO^+	HCS^+	$HCNH^+$	HC_2NC	HC_2CHO	C_6H^-	CH_2CCHCN	C_3H_6		SiS	NH_2	H_2O_2	CH_3Cl 2017
CP	HOC^+	HNCO	HCOOH	NH_2CHO	CH_3NCO	H_2NCH_2CN	CH_3CH_2SH (?)		CS	H_3^+ (•)	C_3H^+	
SiC	H_2O	HNCS	H_2CNH	C_5N	HC_5O 2017	CH_3CHNH	CH_3NHCHO ? 2017		HF	SiCN	HMgNC	
									HD	AlNC	HCCO	
HCl	H_2S	$HOCO^+$	H_2C_2O	*l*-HC_4H *		CH_3SiH_3 2017	HC_7O 2017		FeO ?	SiNC	CNCN 2018	
KCl	HNC	H_2CO	H_2NCN	*l*-HC_4N					O_2	HCP		
									CF^+	CCP		
NH	HNO	H_2CN	HNC_3	*c*-H_2C_3O					SiH ?	AlOH		
NO	MgCN	H_2CS	SiH_4 *	H_2CCNH (?)					PO	H_2O^+		
NS	MgNC	H_3O^+	H_2COH^+	C_5N^-					AlO	H_2Cl^+		
									OH^+	KCN		
NaCl	N_2H^+	*c*-SiC_3	C_4H^-	HNCHCN					CN^-	FeCN		
									SH^+	HO_2		
OH	N_2O	CH_3 *	HC(O)CN	SiH_3CN 2017					SH	TiO_2		
									HCl^+	C_2N		
PN	NaCN	C_3N^-	HNCNH	C_5S (?)					TiO	Si_2C		
									ArH^+	HS_2 2017		
SO	OCS	PH_3	CH_3O						N_2	HCS 2018		
SO^+	SO_2	HCNO	NH_4^+									

Extragalactic Molecules (11/2017; Koln list)

2 atoms	3 atoms	4 atoms	5 atoms	6 atoms	7 atoms	8 atoms	>8 atoms
OH	H_2O	H_2CO	*c*-C_3H_2	CH_3OH	CH_3CCH	HC_6H	*c*-C_6H_6 *
CO	HCN	NH_3	HC_3N	CH_3CN	CH_3NH_2		C_{60}* (?)
H_2 *	HCO^+	HNCO	CH_2NH	HC_4H *	CH_3CHO		
CH	C_2H	C_2H_2 *	NH_2CN	$HC(O)NH_2$			
CS	HNC	H_2CS ?	*l*-C_3H_2				
CH^+	N_2H^+	$HOCO^+$	H_2CCN				
CN	OCS	*c*-C_3H	H_2CCO				
SO	HCO	H_3O^+	C_4H				
SiO	H_2S	*l*-C_3H					
CO^+	SO_2						
NO	HOC^+						
NS	C_2S						
NH	H_2O^+						
OH^+	HCS^+						
HF	H_2Cl^+						
SO^+	NH_2						
ArH^+							
CF^+ 2016							
SH^+ 2017							

Quick Picker

- [x] CO v = 0
- [ ] ^{13}CO v = 0
- [ ] C^{17}O
- [ ] C^{18}O
- [ ] CH$_3$OH vt = 0
- [ ] H$_2$CO
- [ ] HCN v = 0
- [x] HNC v = 0
- [ ] H^{13}CN v = 0
- [ ] HC^{15}N v = 0
- [ ] DCN v = 0
- [x] HCO$^+$ v = 0
- [ ] CS
- [ ] H^{13}CO$^+$
- [ ] NH$_3$
- [ ] C I
- [x] C II
- [ ] O I
- [ ] O III
- [ ] N II
- [ ] H$_2$O v = 0
- [ ] HDO
- [ ] SiO v = 0

splatalogue
database for astronomical spectroscopy

Search:

Telescope Bands: Any / ALMA Band 3 (84-116 GHz) / ALMA Band 4 (125-163 GHz)

Redshift:

Energy Range: Min Max (•) E_L (cm^{-1}) ( ) E_L (K)

Frequency Range: Frequency Unit: GHz

Min 84 Max 750

+ Frequency - Frequency

Search

Astronomical Filters

(Double click to unselect)

- ( ) Top 20 list
- ( ) Planetary Atmosphere
- ( ) Hot Cores
- ( ) Dark Clouds
- ( ) Diffuse Clouds
- ( ) Comets
- ( ) AGB/PPN/PN
- ( ) Extragalactic

Scan to Mobile Splat

Found 22 lines from 84 - 750 GHz, showing 1 - 22
Click on the chemical formula below for more information about that species.

	Species	Chemical Name	Ordered Freq (GHz) (rest frame, redshifted)	Resolved QNs	CDMS/JPL Intensity	Lovas/AST Intensity	E_L (cm^{-1})	E_L (K)	Linelist
1	HCO$^+$ v=0	Formylium	89.18853, 89.18853	1 - 0	0.00000	10.8	0.0000	0.0000	SLAIM
2	HNC v=0	Hydrogen Isocyanide	90.66356, 90.66356	J= 1 - 0	0.00000	1.6	0.0000	0.0000	SLAIM
3	CO v = 0	Carbon Monoxide	115.27120, 115.27120	1- 0	0.00000	60.0	0.0000	0.0000	SLAIM
4	HCO$^+$ v=0	Formylium	178.37507, 178.37507	2 - 1	0.00000		2.9750	4.2803	SLAIM
5	HNC v=0	Hydrogen Isocyanide	181.32473, 181.32473	J= 2 - 1	0.00000		3.0240	4.3508	SLAIM
6	CO v = 0	Carbon Monoxide	230.53800, 230.53800	2- 1	0.00000	70.	3.8450	5.5321	SLAIM
7	HCO$^+$ v=0	Formylium	267.55763, 267.55763	3 - 2	0.00000	12.	8.9250	12.8410	SLAIM
8	HNC v=0	Hydrogen Isocyanide	271.98111, 271.98111	J= 3 - 2	0.00000	10.	9.0730	13.0539	SLAIM
9	CO v = 0	Carbon Monoxide	345.79599, 345.79599	3- 2	0.00000	70.00	11.5350	16.5962	SLAIM
10	HCO$^+$ v=0	Formylium	356.73424, 356.73424	4 - 3	0.00000	17.40	17.8500	25.6820	SLAIM
11	HNC v=0	Hydrogen Isocyanide	362.63030, 362.63030	J= 4 - 3	0.00000	3.0	18.1450	26.1065	SLAIM
12	HCO$^+$ v=0	Formylium	445.90291, 445.90291	5 - 4	0.00000		29.7490	42.8019	SLAIM
13	HNC v=0	Hydrogen Isocyanide	453.26991, 453.26991	J= 5 - 4	0.00000		30.2410	43.5098	SLAIM
14	CO v = 0	Carbon Monoxide	461.04077, 461.04077	4- 3	0.00000	60.	23.0690	33.1910	SLAIM
15	HCO$^+$ v=0	Formylium	535.06164, 535.06164	6 - 5	0.00000		44.6230	64.2022	SLAIM
16	HNC v=0	Hydrogen Isocyanide	543.89755, 543.89755	J= 6 - 5	0.00000		45.3600	65.2625	SLAIM
17	CO v = 0	Carbon Monoxide	576.26793, 576.26793	5- 4	0.00000		38.4480	55.3178	SLAIM
18	HCO$^+$ v=0	Formylium	624.20846, 624.20846	7 - 6	0.00000	14.3	62.4710	89.8813	SLAIM
19	HNC v=0	Hydrogen Isocyanide	634.51082, 634.51082	J= 7 - 6	0.00000	14.8	63.5030	91.3661	SLAIM
20	CO v = 0	Carbon Monoxide	691.47308, 691.47308	6- 5	0.00000	100.	57.6700	82.9738	SLAIM
21	HCO$^+$ v=0	Formylium	713.34137, 713.34137	8 - 7	0.00000	24.7	83.2920	119.8379	SLAIM
22	HNC v=0	Hydrogen Isocyanide	725.10732, 725.10732	J= 8 - 7	0.00000		84.6680	121.8177	SLAIM

Summary

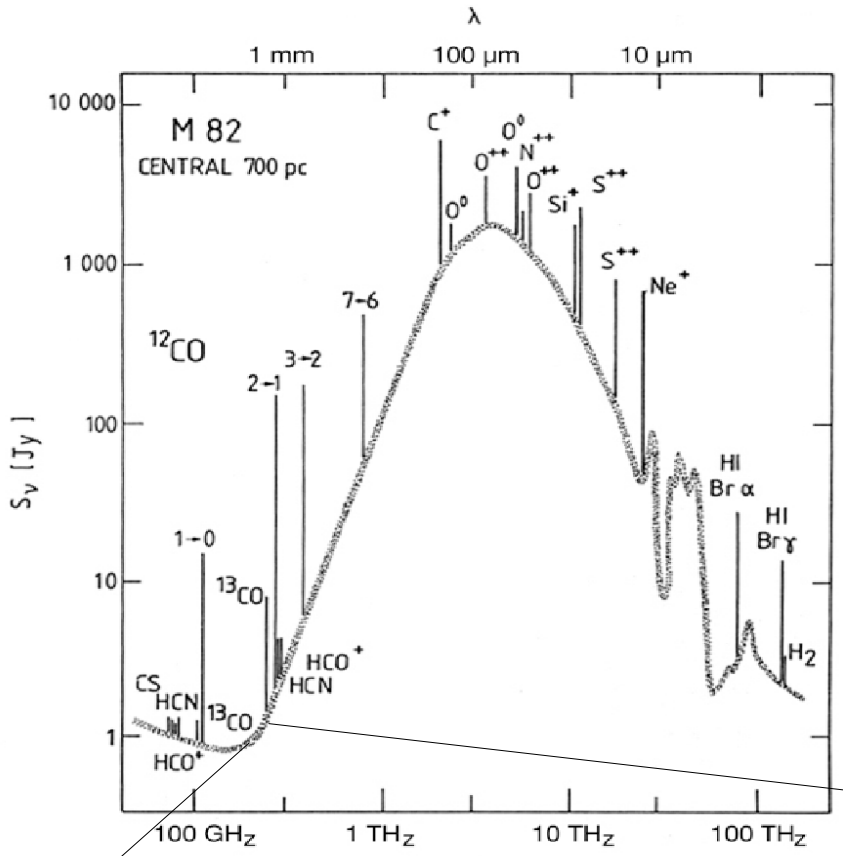

- Continuum is dominated by dust and synchrotron

- CO is the second most abundant molecule after H2
- HCN and HCO+ are high density tracers and relative abundances help distinguish AGN-SB

- CII is the brightest line of nearly all galaxies and PDR tracer
- NII and OII are tracers of cloud metallicity

- Organic molecules are typically associated to young stellar objects
- SiO, CH3OH, H2O are shock tracers